Interference Subspace Rejection: A Framework for Multiuser Detection in Wideband CDMA

Sofiène Affes, *Associate Member, IEEE*, Henrik Hansen, and Paul Mermelstein, *Fellow, IEEE*

***Abstract*—We present a unifying framework for a new class of receivers that employ *linearly-constrained* interference cancellation (IC). The associated multiuser detectors operate in various modes and options ranging in performance from that of IC detectors to that of linear receivers, yet provide more attractive performance/complexity tradeoffs. They exploit both space and time diversities as well as the array-processing capabilities of multiple antennas and carry out simultaneous channel and timing estimation, signal combining and interference rejection. Additionally, they can operate on both links and in multiple mixed-rate traffic scenarios. The improved performance can be translated to increased utilization of wideband code division multiple access networks, particularly at high data rates.**

***Index Terms*—Interference rejection, multiuser detection, smart antennas, space–time processing, spread spectrum multiple access, suppression or cancellation, wideband code division multiple access.**

I. Introduction

THIRD GENERATION wireless systems will deploy wideband code division multiple access (CDMA) [1], [2] access technology to achieve data transmission at variable rates with different mobility and quality of service (QoS) requirements. Standards [1] call for increasing the transmission rate from the 14.4 kb/s voice rate currently supported up to 384 kb/s for mobile users and 2 Mb/ps for portable terminals. Current industrial concerns are how to provide such multirate services in the broadband channels of 5–15 MHz likely to become available. Significant improvement in spectrum efficiency stands out as a key requirement.

The call capacity of wireless CDMA systems is limited by the interference generated by transmissions to/from other mobiles within and outside the cell. On the up-link the interference is mainly that from other transmitting mobiles. Power control attempts to maintain the received powers at values that balance the interference observed by the various mobiles, however, fading and mobility contribute to produce excessive interference in many cases. Where mobiles with different transmission rates are supported within the same cell, the high-rate mobiles manifest strong interference to the low-rate mobiles. On the downlink, transmissions from base stations of other cells, as well as strong interference from the same base to other mobiles, may result in strong interference to the intended signal. Downlink power control may be imprecise or absent altogether. In all these so called near–far problem cases, we can improve the transmission quality or reduce the transmitted power by reducing the interference. In turn, for the same transmission quality, the number of calls supported within the cell may be increased, resulting in improved spectrum utilization.

Power control is presently used to minimize the near–far problem when traffic is equal-rate equal SIR. Mixed-rate traffic will require tight power control to achieve the target SIRs but power differences will remain. Multiuser detectors implement interference cancellation to provide potential benefits such as improvements in capacity and reduced precision requirements for power control. However, these detectors may not be cost-effective to build with a sufficient performance gain over present-day systems [3], [4]. Reaching a satisfactory performance/complexity tradeoff remains a prime concern.

The complexity of the optimal maximum-likelihood sequence detector (MLSD) [5] is exponential in the number of interfering signals to be cancelled, which makes its implementation impractical for large numbers of interferers. Alternative suboptimal detectors fall into two groups: linear and subtractive. Among the linear detectors, the decorrelator [6]–[8] and the minimum mean square error (MMSE) detector [9], [10] offer high near–far resistance. The processing burden for both still presents implementation difficulties. Subtractive IC detectors take the form of parallel interference cancellers (PIC) [11], [12] or successive interference cancellers (SIC) [12], [13]. They offer reduced complexity but suffer from sensitivity to hard decision errors in the feedback of reconstructed signals. The hybrid zero-forcing (ZF) decision-feedback (DF) detector [14] combines a partial linear decorrelator with a SIC-type detector and thereby avoids noise enhancement due to full decorrelation. However, it inherits the complexity of linear receivers and the sensitivity of IC methods to estimation errors.

In the alternative solution proposed here, we upgrade the spatio-temporal array-receiver (STAR) [15], a single-user receiver, by incorporating multiuser detection by interference subspace rejection (ISR) at the signal combining step [16], [17]. The upgraded multiuser receiver STAR-ISR offers different modes that range in performance between IC detectors and linear receivers and require increasing complexity for implementation. At the low end, STAR-ISR reconstructs the interference from channel and data hard decision estimates, then

Manuscript received October 21, 2000; revised June 3, 2001 and November 1, 2001. This work was supported by the Bell/Nortel/NSERC Industrial Research Chair in Personal Communications and by the NSERC Research Grants Program. This paper was presented in part at IEEE ICC'2001, Helsinki, Finland, June 11–14, 2001, and GLOBECOM'2001, San Antonio, TX, November 25–29, 2001.

S. Affes and P. Mermelstein are with INRS-Télécommunications, Université du Québec, Montréal, QC, H5A 1C6 Canada (e-mail: affes @inrs-telecom.uquebec.ca; mermel@inrs-telecom.uquebec.ca).

H. Hansen was with the Technical University of Denmark, Lyngby, Denmark. He is now with L. M. Ericsson A/S, DK-1790 Copenhagen V, Denmark (e-mail: Henrik.hehn.Hansen@lmd.ericsson.se).

Publisher Item Identifier S 0733-8716(02)01009-0.

suppresses it like IC methods. ISR avoids the error-sensitive subtraction and implements instead a more near–far resistant *linearly-constrained* nulling at a complexity comparable to IC. Compared to the linear receivers at the high end, STAR-ISR implements nulling along different interference subspace decompositions with much-reduced complexity. It fully exploits both space and time diversities as well as the array-processing capabilities of multiple antennas while carrying out simultaneous channel and timing estimation, signal combining and interference rejection.

A similar approach to interference cancellation on the downlink of wideband CDMA systems has been proposed by Madkour *et al.* [18], [19]. They provide support for use of suppression by projection as opposed to direct signal cancellation, as well as recognize the advantages of orthogonal projection to the space of interfering signals as opposed to the space of the summed interfering signal. They also require iterative interference cancellation to achieve acceptable performance whereas in our work good performance is achieved even with one-shot cancellation that is much less complex to implement.

The main contribution of this paper is the unified framework for a class of suppression techniques differing in performance and complexity. We provide comparative results in the presence of realistic channel estimation performance achieved by the STAR receiver. With RAKE-type receivers [20] providing degraded channel tracking [21], weaker interference suppression results are achieved.

The interference suppression techniques presented here enable cellular networks to support a wide range of transmission rates. By suppressing the interference generated by high-power high-rate transmissions, weak-power low-rate transmissions can be protected from excessive interference at the same receiving base station. At the same time, the techniques permit a relaxation of the power-control requirements for same-rate users. Interfering transmissions may be suppressed, whether intended to be received at the same or neighboring base stations, as long as their spreading codes are known to the suppressing receiver.

The paper is organized as follows: We develop the data model and position the problem of interference rejection in Section II. In Section III, we introduce ISR and propose various structures and options that cover multiple applications in wideband CDMA. In Section IV, we discuss the advantages of ISR and compare them to previous achievements in multiuser detection. Simulations are found in Section V. Finally, we draw conclusions in Section VI. The conclusions of Section VI suggest that the simplest STAR-ISR techniques are implementable today and offer significant capacity improvements.

II. Data Model and Formulation of the Problem

A. General Assumptions and Model

We consider the up-link of an asynchronous cellular CDMA system where each base station is equipped with a receiving antenna-array of M sensors. Application to the downlink will be studied in a future work [22]. For the sake of simplicity, we assume for now that all users transmit with the same modulation and at the same rate. We also assume that the base station knows the spreading codes of all the terminals with which it communicates. The phase-shift keying (PSK) symbol sequence for a mobile with index u is first differentially encoded[1] at the rate $1/T$, where T is the symbol duration. The resulting differential phase-shift keying (DPSK) sequence $b^u(t)$ is then spread by a personal pseudorandom noise (PN) code $c^u(t)$ at a rate $1/T_c$, where T_c is the chip pulse duration. The processing gain is given by $L = T/T_c$. We assume the use of long codes. Other extensions regarding assumptions and applications will be discussed later. We write the spreading-code segment over the nth period T as

$$c_n^u(t) = \sum_{l=0}^{L-1} c_{n,l}^u \phi(t - lT_c - nT) \tag{1}$$

where $c_{n,l}^u = \pm 1$ for $l = 0, \ldots, L-1$, is a random sequence of length L and $\phi(t)$ is the chip pulse. Finally, we assume a multipath fading environment with P resolvable paths, where the delay spread $\Delta\tau$ is small compared to the symbol duration (i.e., $\Delta\tau \ll T$).

At time t, the observation vector received by the antenna array of one particular cell can be written as follows:

$$X(t) = \sum_{u=1}^{U} \psi^u(t) X^u(t) + N^{\text{th}}(t) \tag{2}$$

where U is the total number of mobiles received at the selected base station from inside and outside the cell, $X^u(t)$ is the received signal vector from the mobile u, $\psi^u(t)$ is its total received amplitude, and $N^{\text{th}}(t)$ is the thermal noise received at each antenna element. The contribution $X^u(t)$ of the uth mobile to the observation vector $X(t)$ is given by[2]

$$\begin{aligned} X^u(t) &= H^u(t) \otimes c^u(t) b^u(t) \\ &= \sum_{p=1}^{P} G_p^u(t) \varepsilon_p^u(t) b^u\left(t - \tau_p^u(t)\right) c^u\left(t - \tau_p^u(t)\right) \end{aligned} \tag{3}$$

where $H^u(t)$ is the channel response vector from the mobile to the antenna elements and $\otimes$ denotes time-convolution. In the right-hand term of (3), the propagation time-delays along the P paths $\tau_p^u(t) \in [0, T), p = 1, \ldots, P$, are chip-asynchronous [15], $G_p^u(t) = [G_{1,p}^u(t), \ldots, G_{M,p}^u(t)]^T$ are the propagation vectors and $\varepsilon_p^u(t)^2$ are the power fractions along each path of the total power $\psi^u(t)^2$ received from the uth mobile (i.e., $\sum_{p=1}^{P} \varepsilon_p^u(t)^2 = 1$). The received power is affected by path loss, Rayleigh fading, and shadowing. We assume that $G_p^u(t), \varepsilon_p^u(t)^2$ and $\psi^u(t)^2$ vary slowly and neglect their variation over Q symbol durations (i.e., QT).

[1]Differential coding enables use of STAR without a pilot [15] for blind channel identification and quasicoherent detection with differential decoding. It hence avoids noncoherent demodulation [23]. A reduced-power pilot can be used to avoid differential coding and decoding [24] while orthogonal modulation [13], [25] can be detected coherently by STAR without a pilot [26].

[2]Note that the model described is baseband without loss of generality. Both the carrier frequency modulation and demodulation steps can be embedded in the chip pulse-shaping and matched-filtering operations of (1) and (4), respectively.

In successive overlapping frames of period QT, we define the matched-filtering observation vector for frame number n over the time interval $[0,(Q+1)T)$ by

$$Y_n(t)=\frac{1}{T_c}\int_{D_\phi} X(aQT/2+nQT+t+t')\phi(t')\,dt' \quad (4)$$

where D_ϕ denotes the temporal support[3] of $\phi(t)$ and $a\in\{0,1\}$ stands for a possible time-shift by $QT/2$ to avoid locating the frame edges in the middle of the delay spread [15]. For simplicity, we assume $a=0$. After sampling at the chip rate and framing over $(Q+1)L$ chip samples at the symbol rate, we obtain the $M\times((Q+1)L)$ matched-filtering observation matrix

$$\mathbf{Y}_n=[Y_n(0),Y_n(T_c),\ldots,Y_n(((Q+1)L-1)T_c)]. \quad (5)$$

It can be expressed as

$$\mathbf{Y}_n=\sum_{u=1}^{U}\psi_n^u\mathbf{Y}_n^u+\mathbf{N}_n^{\rm pth} \quad (6)$$

where the base-band preprocessed thermal noise (i.e., after matched-pulse filtering) contributes

$$\mathbf{N}_n^{\rm pth}=[N^{\rm pth}(nQT),N^{\rm pth}(nQT+T_c),\ldots, N^{\rm pth}(nQT+((Q+1)L-1)T_c)] \quad (7)$$

$\psi_n^u=\psi^u(nQT)$ and each user u contributes its user-observation matrix $\mathbf{Y}_n^u$, obtained by

$$\mathbf{Y}_n^u=[Y_n^u(0),Y_n^u(T_c),\ldots,Y_n^u(((Q+1)L-1)T_c)] \quad (8)$$

$$Y_n^u(t)=\frac{1}{T_c}\int_{D_\phi} X^u(nQT+t+t')\phi(t')\,dt'. \quad (9)$$

B. Parametric Data Decompositions

In the following, we detail the structure of the user-observation matrix $\mathbf{Y}_n^u$ along various parametric data decompositions that will serve later as new interference characterizations for use by a new class of interference cancellers.

First, we decompose $\mathbf{Y}_n^u$ over the symbols from uth user that contribute to its data as follows:

$$\mathbf{Y}_n^u=\sum_{k=-1}^{Q} b_{nQ+k}^u\mathbf{Y}_{k,n}^u=b_{nQ+k}^u\mathbf{Y}_{k,n}^u+\mathbf{I}_{{\rm ISI},n}^{u,k} \quad (10)$$

where $b_k^u=b^u(kT)$ and where the canonic user-observation matrices $\mathbf{Y}_{k,n}^u$ are given by

$$\mathbf{Y}_{k,n}^u=\left[Y_{k,n}^u(0),Y_{k,n}^u(T_c),\ldots,Y_{k,n}^u(((Q+1)L-1)T_c)\right] \quad (11)$$

$$Y_{k,n}^u(t)=\frac{1}{T_c}\int_{D_\phi} X_{k,n}^u(nQT+t+t')\phi(t')\,dt' \quad (12)$$

$$X_{k,n}^u(t)=H(t)\otimes c_{nQ+k}^u(t). \quad (13)$$

Due to asynchronism and multipath propagation, each user-observation matrix carries information from the Q current (i.e., $k=0,\ldots,Q-1$) as well as from the previous (i.e., $k=-1$) and future (i.e., $k=Q$) block symbols of the corresponding user. It can be decomposed by separating the contributions of $Q+2$ consecutive symbols so as to isolate each of the Q desired symbols with index say $k\in\{0,\ldots,Q-1\}$ and yet overcome inter-symbol interference (ISI) of the uth user over its kth symbol defined as

$$\mathbf{I}_{{\rm ISI},n}^{u,k}=\sum_{\substack{k'=-1\\k'\neq k}}^{Q} b_{nQ+k'}^u\mathbf{Y}_{k',n}^u. \quad (14)$$

As an alternative to the decomposition over symbols of (10), we can separate $\mathbf{Y}_n^u$ over contributions from the $N_f=MP$ diversity branches or fingers as

$$\mathbf{Y}_n^u=\sum_{f=1}^{N_f}\zeta_{f,n}^u\mathbf{Y}_n^{u,f} \quad (15)$$

where finger $f=(p-1)M+m$, denotes antenna $m\in\{1,\ldots,M\}$ and propagation path $p\in\{1,\ldots,P\}$ and $\zeta_{f,n}^u=G_{m,p}^u(nQT)\varepsilon_p^u(nQT)$ stands for the corresponding propagation coefficient. Each diversity-observation matrix $\mathbf{Y}_n^{u,f}$ is defined as

$$\mathbf{Y}_n^{u,f}=\left[Y_n^{u,f}(0),Y_n^{u,f}(T_c),\ldots,Y_n^{u,f}(((Q+1)L-1)T_c)\right] \quad (16)$$

$$Y_n^{u,f}(t)=\frac{1}{T_c}\int_{D_\phi} X^{u,f}(nQT+t+t')\phi(t')\,dt' \quad (17)$$

$$X^{u,f}(t)=\mathbb{1}_M^m\delta\left(t-\tau_p^u(t)\right)\otimes b^u(t)c^u(t) \quad (18)$$

where $\mathbb{1}_M^m=[0,\ldots,0,1,0,\ldots,0]^T$ is a $M\times 1$ vector of zeros except for one at the mth element and $\delta(t)$ is the Dirac impulse.

The two decompositions of the user-observation matrix (i.e., over symbols or diversity branches) can be combined as follows:

$$\mathbf{Y}_n^u=\sum_{k=-1}^{Q}\sum_{f=1}^{N_f} b_{nQ+k}^u\zeta_{f,n}^u\mathbf{Y}_{k,n}^{u,f} \quad (19)$$

where the canonic diversity-observation matrix $\mathbf{Y}_{k,n}^{u,f}$ is given by

$$\mathbf{Y}_{k,n}^{u,f}=\left[Y_{k,n}^{u,f}(0),Y_{k,n}^{u,f}(T_c),\ldots,Y_{k,n}^{u,f}(((Q+1)L-1)T_c)\right] \quad (20)$$

$$Y_{k,n}^{u,f}(t)=\frac{1}{T_c}\int_{D_\phi} X_{k,n}^{u,f}(nQT+t+t')\phi(t')\,dt' \quad (21)$$

$$X_{k,n}^{u,f}(t)=\mathbb{1}_M^m\delta\left(t-\tau_{p,n}^u\right)\otimes c_{nQ+k}^u(t) \quad (22)$$

where $\tau_{p,n}^u=\tau_p^u(nQT)$. Hence, one can easily derive the following identities

$$\mathbf{Y}_n^{u,f}=\sum_{k=-1}^{Q} b_{nQ+k}^u\mathbf{Y}_{k,n}^{u,f} \quad (23)$$

$$\mathbf{Y}_{k,n}^u=\sum_{f=1}^{N_f}\zeta_{f,n}^u\mathbf{Y}_{k,n}^{u,f}. \quad (24)$$

In the next section, we shall use the above parametric data decompositions to derive a new class of interference cancellers. Before we do so, we formulate the interference suppression problem.

C. Formulation of the Problem and Background

Power mismatch (i.e., near–far situations) arises on the up-link unintentionally due to imperfect power control for path loss and shadowing variations, and intentionally when we

[3]For a rectangular pulse, D_ϕ is $[0,T_c]$. In practice, it is the temporal support of a truncated square-root raised cosine.

increase the power of particular users (e.g., "priority links," acquisition, higher order modulations or higher data rates in mixed-rate traffic). We assume that power control is used on the up-link to reduce the power mismatch between users and identify two generic situations where application of multiuser detection is of interest. The first is a homogeneous traffic situation comprising high-power high data-rate links with roughly equal powers, where each user attempts to suppress transmissions from the others. The second is a mixed-rate traffic situation where a low-power low-rate user attempts to eliminate interference from high-power high-rate users, each power level being set to meet the QoS of the corresponding rate. Any other suppression scenario of interest boils down to a combination of these two generic cases (see Section III-D). Suppression of a low-power low-rate user likely offers only modest performance gain and, hence, is given the lowest processing priority within the computational power available (see discussion of complexity in Section V-C).

For the sake of simplicity, we formulate the problem of multiuser detection in the mixed-rate traffic scenario.[4] Later in Section III-C we address the homogeneous case. We hence divide the mobiles received at a base station into two subsets, one comprising those whose received signal powers are relatively high and a second whose powers are relatively low. Assume the presence of NI strong interfering mobiles in the first subset and assign them the indices $i = 1, \ldots, NI$. Consider a desired user with index d in the second subset, and formulate the suppression problem with respect to each of his Q symbols to be detected in each frame (i.e., detect Q data symbols of user d in parallel based on a single observation $\mathbf{Y}_n$).

Using the data decompositions of the previous section and defining for convenience of notation a vector $\underline{V}$ as a matrix $\mathbf{V}$ reshaped columwise, we rewrite the vectorized matched-filtering observation matrix $\mathbf{Y}_n$ of (6) for user d and for $k = 0, \ldots, Q-1$ as

$$\underline{Y}_n = \psi_n^d b_{nQ+k}^d \underline{Y}_{k,n}^d + \left\{ \sum_{i=1}^{NI} \psi_n^i \underline{Y}_n^i \right\} + \left\{ \underline{I}_{\mathrm{ISI},n}^{d,k} + \sum_{\substack{u=NI+1 \\ u \neq d}}^{U} \psi_n^u \underline{Y}_n^u + \underline{N}_n^{\mathrm{pth}} \right\} \tag{25}$$

$$= s_n^{d,k} \underline{Y}_{k,n}^d + \underline{I}_n + \underline{N}_n^{d,k} \simeq s_n^{d,k} \underline{Y}_{k,n}^d + \underline{I}_n + \underline{N}_n \tag{26}$$

where $s_n^{d,k} = \psi_n^d b_{nQ+k}^d$ denotes the kth signal component of the desired user and

$$\underline{I}_n = \sum_{i=1}^{NI} \psi_n^i \underline{Y}_n^i = \sum_{i=1}^{NI} \psi_n^i \sum_{f=1}^{N_f} \zeta_{f,n}^i \underline{Y}_n^{i,f} = \sum_{i=1}^{NI} \psi_n^i \sum_{k'=-1}^{Q} b_{nQ+k'}^i \underline{Y}_{k',n}^i = \sum_{i=1}^{NI} \psi_n^i \sum_{f=1}^{N_f} \sum_{k'=-1}^{Q} b_{nQ+k'}^i \zeta_{f,n}^i \underline{Y}_{k',n}^{i,f} \tag{27}$$

[4]We assume for simplicity that all users transmit with the same symbol-rate and that only differences between their modulation orders cause noticeable power mismatch. Extension of our suppression techniques to the mixed symbol-rate scenario is *ad hoc*.

is part of the multiple access interference (MAI) vector to be suppressed. The noise vector $\underline{N}_n^{d,k}$ comprises ISI from the desired user over its kth symbol, the rest of the MAI from all other users in the system, and the preprocessed thermal noise. For convenience of notation, $\underline{N}_n^{d,k}$ or simply $\underline{N}_n$ is assumed to be uncorrelated[5] both in space and time with variance σ_N^2. Later we address explicit ISI suppression and discuss other extensions to the correlated noise case (see Sections III-D and E).

Single-user receivers such as the RAKE/2D-RAKE [27] or STAR [15] regard the partial MAI vector $\underline{I}_n$ as another contribution to the noise $\underline{N}_n$ and, hence, implement spatio-temporal maximum ratio combining (MRC). For instance, STAR implements MRC for $k = 0, \ldots, Q-1$ as follows:[6]

$$\hat{s}_n^{d,k} = \mathrm{W}_{\mathrm{MRC},n}^{d,k^H} \underline{Y}_n = \frac{\hat{\underline{Y}}_{k,n}^{d^H} \underline{Y}_n}{\left\| \underline{Y}_{k,n}^d \right\|^2}. \tag{28}$$

However, MRC is suboptimal despite use of power control on the up-link due to interference correlation from high-power high-rate users in $\underline{I}_n$. We next introduce a new class of interference cancellers that suppress $\underline{I}_n$, and offer a unifying framework for efficient and cost-effective multiuser detection.

III. The Proposed Multiuser Detector

A. Interference Subspace Rejection

In the general case, the total interference $\underline{I}_n$ is an unknown random vector which lies at any moment in an interference subspace spanned by a matrix, say $\mathbf{C}_n$ (i.e., $\underline{I}_n \in \mathrm{Vec}\{\mathbf{C}_n\}$) with dimension N_c which depends on the number of interference parameters [i.e., power, data symbols, multipath components, and delays, see (27)] estimated separately

$$\mathbf{C}_n = \begin{cases} \{\underline{I}_n\} \Big|_{\left\{\psi_n^i, \zeta_{f,n}^i, b_{nQ+k}^i, \tau_{p,n}^i\right\}_{i=1}^{NI}} \\ \left\{\ldots, \underline{Y}_n^i, \ldots\right\}_{i=1}^{NI} \Big|_{\left\{\zeta_{f,n}^i, b_{nQ+k}^i, \tau_{p,n}^i\right\}_{i=1}^{NI}} \\ \left\{\ldots, \underline{Y}_n^{i,f}, \ldots\right\}_{(i,f)=(1,1)}^{(NI,N_f)} \Big|_{\left\{b_{nQ+k}^i, \tau_{p,n}^i\right\}_{i=1}^{NI}} \\ \left\{\ldots, \underline{Y}_{k,n}^i, \ldots\right\}_{(i,k)=(1,-1)}^{(NI,Q)} \Big|_{\left\{\zeta_{f,n}^i, \tau_{p,n}^i\right\}_{i=1}^{NI}} \\ \left\{\ldots, \underline{Y}_{k,n}^{i,f}, \ldots\right\}_{(i,f,k)=(1,1,-1)}^{(NI,N_f,Q)} \Big|_{\left\{\tau_{p,n}^i\right\}_{i=1}^{NI}} \end{cases} . \tag{29}$$

The more interference parameters we estimate, the fewer dimensions N_c (number of constraints) are needed to characterize the interference subspace for suppression. However, the sensitivity of the suppression method to parameter estimation errors also increases. With the above parametric/subspace decompositions of $\underline{I}_n$, we readily identify new performance/complexity tradeoffs for suppression (see Section V-C). As shown in Table I, a number of alternative techniques may be recognized that use different reconstructions of the matrix $\mathbf{C}_n$, referred to as the constraint matrix.

[5]The central limit theorem allows processing the set of low-power low-rate interferers—presumably many such are present—as white noise.

[6]Note that we take the real part of the MRC output if the modulation is BPSK. Other operations in STAR that: 1) estimate the data symbols and the power of the desired user and 2) identify the channel from the signal component $\hat{s}_n^{d,k}$ as shown in Fig. 1 are explained in detail in [15] and [30].

TABLE I
CONSTRAINT MATRIX $\hat{\mathbf{C}}_n$ AND THE CORRESPONDING NUMBER OF CONSTRAINTS OR COLUMNS N_c FOR EACH ISR MODE. EACH GENERIC COLUMN $\hat{\underline{C}}_{j,n}$ SHOWN ABOVE IS NORMALIZED TO 1

ISR Mode	$\hat{\mathbf{C}}_n = \left[\ldots, \hat{\underline{C}}_{j,n}, \ldots\right]$	N_c
Total Realization (TR) (const./total MAI)	$\left[\hat{\underline{I}}_n = \sum_{i=1}^{NI} \hat{\psi}_n^i \hat{\underline{I}}_n^i\right]$	1
Realizations (R) (const./interferer)	$\left[\ldots, \hat{\underline{Y}}_n^i = \left\{ \underbrace{\sum_{f=1}^{N_f} \hat{\zeta}_{f,n}^i \hat{\underline{Y}}_n^{i,f}}_{\text{decompose/fingers}}, \ldots \underbrace{\sum_{k=-1}^{Q} \hat{b}_{nQ+k}^i \hat{\underline{Y}}_{k,n}^i}_{\text{decompose/symbols}} \right.\right]$	NI
Diversities (D) (const./finger/int.)	$\left[\ldots, \hat{\underline{Y}}_n^{i,f} = \sum_{k=-1}^{Q} \hat{b}_{nQ+k}^i \hat{\underline{Y}}_{k,n}^{i,f}, \ldots\right]$	$N_f NI$
Hypotheses (H) (const./sym./int.)	$\left[\ldots, \hat{\underline{Y}}_{k,n}^i = \sum_{f=1}^{N_f} \hat{\zeta}_{f,n}^i \hat{\underline{Y}}_{k,n}^{i,f}, \ldots\right]$	$(Q+2)NI$
Reduced Hypotheses (RH) (const./int./future sym.)	$\left[\ldots, \sum_{k=-1}^{Q-1} \hat{b}_{nQ+k}^i \hat{\underline{Y}}_{k,n}^i, \hat{\underline{Y}}_{Q,n}^i \ldots\right]$	$2NI$
Decorrelator can be regarded as H&D (const./sym./finger/int.)	$\left[\ldots, \hat{\underline{Y}}_{k,n}^{i,f}, \ldots\right]$	$(Q+2)N_f NI$

To suppress $\underline{I}_n$ as characterized in subspace $\mathbf{C}_n$, the combiner for the kth symbol of the desired user, for $k = 0, \ldots, Q-1$, must conform[7] to the following theoretical constraints

$$\begin{cases} \mathrm{W}_n^{d,k^H} \underline{Y}_{k,n}^d = 1, \\ \mathrm{W}_n^{d,k^H} \mathbf{C}_n = 0, \end{cases} \Rightarrow \begin{cases} \mathrm{W}_n^{d,k^H} \underline{Y}_{k,n}^d = 1, \\ \mathrm{W}_n^{d,k^H} \underline{I}_n = 0. \end{cases} \tag{30}$$

The first constraint guarantees a distortionless response to the desired user while the second rejects the interference subspace and thereby cancels the total interference $\underline{I}_n$. We shall refer to this approach as interference subspace rejection (ISR).

A solution for the ISR combiner (i.e., the constrained spatio-temporal combiner) $\underline{W}_n^{d,k}$ is given for $k = 0. \ldots, Q-1$ by

$$\mathbf{Q}_n = \left(\hat{\mathbf{C}}_n^H \hat{\mathbf{C}}_n\right)^{-1} \tag{31}$$

$$\mathbf{\Pi}_n = \mathbf{I}_{N_T} - \hat{\mathbf{C}}_n \mathbf{Q}_n \hat{\mathbf{C}}_n^H \tag{32}$$

$$\underline{W}_n^{d,k} = \frac{\mathbf{\Pi}_n \hat{\underline{Y}}_{k,n}^d}{\hat{\underline{Y}}_{k,n}^{d^H} \mathbf{\Pi}_n \hat{\underline{Y}}_{k,n}^d} \tag{33}$$

where $N_T = M(Q+1)L$ is the total space dimension and $\mathbf{I}_{N_T}$ denotes an $N_T \times N_T$ identity matrix. First, we form the projector[8] $\mathbf{\Pi}_n$ orthogonal to the constraint matrix estimate $\hat{\mathbf{C}}_n$. Second, we project the estimated response vector $\hat{\underline{Y}}_{k,n}^d$ and normalize it[9] to derive the ISR combiner $\underline{W}_n^{d,k}$. We use this combiner instead of MRC in (28) to extract the signal component estimates $\hat{s}_n^{d,k}$. An upgrade of the single-user STAR [15], referred to as STAR-ISR, exploits these new ISR outputs as shown in Fig. 1 to improve estimation of the symbol decisions $\hat{b}_{nQ+k}^d$, the received power $(\hat{\psi}_n^d)^2$, and the channel parameters $\{\hat{\zeta}_{f,n}^d, \hat{\tau}_{p,n}^d\}$. An enhanced version of STAR-ISR [30] that incorporates ISR in the channel identification process further improves these estimates and offers an integrated solution for an efficient and cost-effective multiuser receiver in wideband CDMA.

Similar STAR-ISR receivers for each interferer (see Section III-C) estimate $\{\hat{\psi}_n^i, \hat{b}_{nQ+k}^i, \hat{\zeta}_{f,n}^i, \hat{\tau}_{p,n}^i\}$ and enable construction of the constraint matrix $\hat{\mathbf{C}}_n$ (see Fig. 1). An estimate of $\hat{\mathbf{C}}_n$ is constructed with MRC symbol estimates or reconstructed with ISR symbol estimates from previous ISR stages in a multistage processing scheme (see Fig. 2 and Section III-G). In Table I, we show how to form $\hat{\mathbf{C}}_n$ for different modes, which decompose or regroup interference vectors from the different interference subspace characterizations of (29). The total realization (TR) mode nulls the total interference vector and, hence, requires accurate estimation of all the channel and data parameters of the NI interferers. It is similar to the PIC detector, only it implements the more accurate nulling instead of the subtraction of $\underline{I}_n$. As one example, ISR-TR would still implement a perfect null-constraint if the power estimates were all biased by an identical multiplicative factor, while interference cancellers would subtract the wrong amount of interference. The realizations (R) mode nulls the signal vector of each interferer and, hence, becomes even more robust to power estimation errors. The diversities (D) mode nulls the signal vector from each interfering finger of each interferer and, hence, gains additional robustness to channel estimation errors. The hypotheses (H) mode nulls the signal vector from each interfering symbol of each interferer and, hence, introduces robustness to data estimation errors. In contrast to previous modes referred to as decision feedback (DF) modes, the H mode does not feed back decisions from the symbol estimates into $\hat{\mathbf{C}}_n$. Its combiner coefficients are hence symbol-independent and can be computed less frequently when the channel time-variations are slow and when the codes are short. Finally, the reduced hypotheses (RH) mode, a hybrid between the R and H modes, reduces the number of constraints N_c (i.e., computational cost) from $(Q+2)NI$ for the H mode to just $2NI$.

In fact, the H mode is not the most expensive in complexity. Combination of the H and D modes results in a structure similar to the decorrelator[10] which requires a larger number of constraints, i.e., $(Q+2)N_f NI$. One can even introduce a finer decomposition by nulling additional dimensions over possible multipath delays (e.g., over the delay spread) to gain robustness to synchronization errors [21], [31], [32]. However, increasing

[7]This combining approach is borrowed from a multisource (i.e., multiuser) beamforming method called the adaptive source-subspace extraction and tracking (ASSET) technique [28], [29], an early array-processing form of a group ZF, MMSE, or hybrid ZF-MMSE detector.

[8]This projector is computed once for all for all desired users at the cost of a single inversion of an $N_c \times N_c$ matrix. In the D mode in particular (see Table I), the matrix is sparse because $\hat{\underline{Y}}_n^{i,f}$ is nonzero only at elements $m, m+M, m+2M, \ldots, m+((Q+1)L-1)M$; and the matrix inversion boils down to M inversions of $PNI \times PNI$ matrices or even to one inversion only when delays of a given propagation path are the same at all antennas as assumed herein.

[9]These operations actually exploit redundant or straightforward computations in the data projection and the normalization.

[10]The use of decision feedback with the decorrelator is already well documented (e.g., [14]); but only past symbols were fed back in previous works. In ISR DF modes, past, present, and future symbols are all fed back.

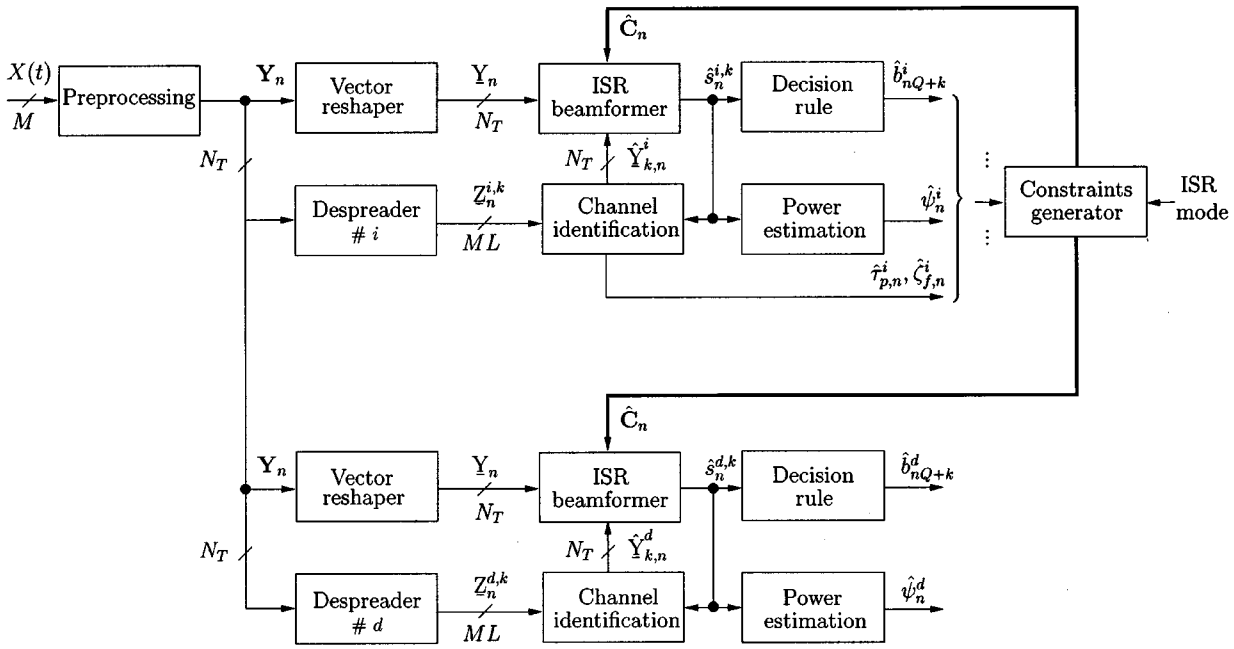

Fig. 1. Block diagram of STAR-ISR.

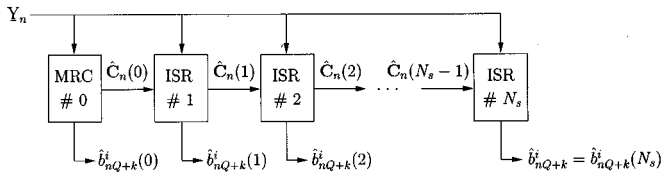

Fig. 2. Block diagram of multistage ISR processing $(\mathrm{BER}(N_s) \leq \mathrm{BER}(N_s-1) \leq \cdots \leq \mathrm{BER}(0))$.

the number of constraints N_c not only increases complexity but also results in more severe noise enhancement when N_c approaches the total dimension $N_T = M(Q+1)L$ of the entire observation space.

To reduce complexity, guarantee stability in the matrix inversion of (31) if it becomes close to rank-degenerate, and minimize noise enhancement, we replace the constraint matrix $\hat{\mathbf{C}}_n$ in (31) and (32) by the orthonormal interference subspace of rank $N_r \leq N_c$ that spans its column vectors to yield the projector $\mathbf{\Pi}_n = \mathbf{I}_{N_T} - \hat{\mathbf{V}}_n \hat{\mathbf{V}}_n^H$ used in (33), which replaces the matrix inversion by the Gram-Schmidt matrix orthonormalization.[11] In practice, $\hat{\mathbf{V}}_n$ can hardly reflect the true rank of $\hat{\mathbf{C}}_n$ if it is close to degenerate. It corresponds to the subspace of reduced rank $\hat{N}_r$ with the highest interference energy to cancel.

To further minimize noise enhancement, one can also increase the dimension of the observation space $N_T = M(Q+1)L$ by increasing Q. Increasing the frame duration $(Q+1)T$ has the additional advantage of enabling asynchronous processing of a wider interuser delay spread as well as multirate users. In terms of noise enhancement reduction, the DF modes—namely, TR, R, D, and RH—will benefit most from increasing Q because the number of their constraints N_c remains constant. In contrast, the H mode sees its gain saturate. However, while the H mode does not exact a processing delay, the DF modes TR, R, and D will require an increasing delay of Q symbol durations to allow buffering of the next data frame, plus one processing cycle (PC) to allow estimation of $\hat{b}^i_{(n+1)Q}$ (i.e., the first desired symbol from the next frame). The DF mode RH, which directs a null toward $b^i_{(n+1)Q}$ requires only a delay of one processing cycle (1PC) to allow estimation of the interferers' symbols from the current frame. However, the cycle duration also increases with Q.

B. Extending Dimensionality: X-Option

To reduce noise enhancement and to allow processing of completely asynchronous transmissions without exacting larger processing delays in the DF modes, it is possible to increase the frame duration (i.e., the observation dimension) without increasing Q. We simply generalize the observation to include additional past spread data which has already been processed.

If we expand the matched-filtering observation matrix of (5) to include previously processed N_X symbols, the observation becomes

$$\mathbf{Y}_n = [Y_n(-N_X L T_c), \ldots, Y_n(-T_c), Y_n(0), Y_n(T_c), \ldots, Y_n(((Q+1)L-1)T_c)]. \quad (34)$$

Similarly, expanding $\mathbf{Y}_n^u, \mathbf{Y}_{k,n}^u, \mathbf{Y}_n^{u,f}$ and $\mathbf{Y}_{k,n}^{u,f}$ keeps the parametric data decompositions of (6), (15), and (24) unchanged, provided that the expanded frame duration $(N_X+Q+1)T$ remains below the coherence time of the channel. On the other hand, decompositions of (10), (14), (19), and (23) that isolate contributions over symbols extend the first summation index

[11]Note that orthonormalization becomes unnecessary if we check that $\hat{\mathbf{C}}_n$ is close to orthonormal (i.e., $\hat{\mathbf{C}}_n \simeq \hat{\mathbf{V}}_n$).

over past symbols from -1 to $-(N_X+1)$. These extended decompositions may be better illustrated by rewriting the interference characterization of (27) as

$$\begin{aligned}\underline{I}_n &= \sum_{i=1}^{NI}\psi_n^i\underline{Y}_n^i = \sum_{i=1}^{NI}\psi_n^i\sum_{f=1}^{N_f}\zeta_{f,n}^i\underline{Y}_n^{i,f}\\ &= \sum_{i=1}^{NI}\psi_n^i\sum_{k=-N_X-1}^{Q} b_{nQ+k}^i\underline{Y}_{k,n}^i\\ &= \sum_{i=1}^{NI}\psi_n^i\sum_{f=1}^{N_f}\sum_{k=-N_X-1}^{Q} b_{nQ+k}^i\zeta_{f,n}^i\underline{Y}_{k,n}^{i,f}. \end{aligned}\tag{35}$$

From the above decompositions of $\underline{I}_n$, the definition of the constraint matrix $\mathbf{C}_n$ in Table I remains the same for the DF modes, although its construction requires now summation over estimated symbols $\hat{b}_{nQ+k}^i$ starting with index $k=-N_X-1$ instead of $k=-1$.

Although the X-option is tailored to the DF modes of ISR, it could be applied to the H mode using $(N_X+Q+2)NI$ constraints. However, increasing Q achieves the same benefits while it enables processing of more symbols in a block with minimum overlap between processed frames. Instead, the X-option can combine the H mode in another variant of the hybrid RH mode using the following constraint matrix with number of constraints $N_c=(Q+2)NI$

$$\mathbf{C}_n=\left[\ldots,\sum_{k=-N_X-1}^{-1}\hat{b}_{nQ+k}^i\underline{\hat{Y}}_{k,n}^i,\underline{\hat{Y}}_{0,n}^i,\underline{\hat{Y}}_{1,n}^i,\ldots,\underline{\hat{Y}}_{Q,n}^i,\ldots\right].\tag{36}$$

The above example is one possible hybrid among many other combinations between ISR modes. For lack of space, hybrid ISR modes will not be pursued in the following. Only the generic modes (i.e., TRX, RX, DX, and H) will be studied.

Clearly, extension of the observation space to arrive at a total dimension $N_T=M(N_X+Q+1)L$ provides additional degrees of freedom and results in less white noise enhancement as shown in Section V-B.

C. Joint ISR Detection

Previously, we focused on implementation of ISR for a weak-power low-rate user in mixed-rate traffic. We now address the homogeneous-rate case described in Section II-C and introduce joint ISR detection among strong-power high-rate interferers. It allows for mutual interference rejection with one matrix inversion only. This generic case obviously applies to suppression among interferers in the mixed-rate scenario treated earlier. Here, we simply merge the signal contribution of the dth user into the noise vector $\underline{N}_n$ in (26) and focus on processing the NI users.

TABLE II
SIGNAL BLOCKING MATRIX $\hat{\mathbf{C}}_n^{i,k}$ AND THE CORRESPONDING NUMBER OF CONSTRAINTS OR COLUMNS N_c FOR EACH ISR MODE (N_X IS SET TO 0 IN THE H MODE). $\bar{\delta}_{i',i}^{k',k}=0$ IF $i'=i$ AND $k'=k$, AND 1 OTHERWISE. EACH GENERIC COLUMN $\hat{\mathrm{C}}_{j,n}^{i,k}$ SHOWN ABOVE IS DIVIDED BY THE NORM OF THE CORRESPONDING GENERIC COLUMN $\underline{\hat{C}}_{j,n}$ OF THE CONSTRAINT MATRIX $\hat{\mathbf{C}}_n$ (OBTAINED HERE BY REPLACING $\bar{\delta}_{i',i}^{k',k}$ WITH 1)

ISR Mode	$\hat{\mathbf{C}}_n^{i,k}=\left[\ldots,\underline{\hat{C}}_{j,n}^{i,k},\ldots\right]$	N_c
TRX	$\left[\sum_{i'=1}^{NI}\sum_{f=1}^{N_f}\sum_{k'=-N_X-1}^{Q}\hat{\psi}_n^{i'}\hat{\zeta}_{f,n}^{i'}\hat{b}_{nQ+k}^{i'}\underline{\hat{Y}}_{k',n}^{i',f}\bar{\delta}_{i',i}^{k',k}\right]$	1
RX	$\left[\ldots,\sum_{f=1}^{N_f}\sum_{k'=-N_X-1}^{Q}\hat{\zeta}_{f,n}^{i'}\hat{b}_{nQ+k}^{i'}\underline{\hat{Y}}_{k',n}^{i',f}\bar{\delta}_{i',i}^{k',k},\ldots\right]$	NI
DX	$\left[\ldots,\sum_{k'=-N_X-1}^{Q}\hat{b}_{nQ+k}^{i'}\underline{\hat{Y}}_{k',n}^{i',f}\bar{\delta}_{i',i}^{k',k},\ldots\right]$	N_fNI
H	$\left[\ldots,\sum_{f=1}^{N_f}\hat{\zeta}_{f,n}^{i'}\underline{\hat{Y}}_{k',n}^{i',f}\bar{\delta}_{i',i}^{k',k},\ldots\right]$	$(Q+2)NI$

A combiner $\underline{W}_n^{i,k}$ similar to that of (33) can be derived for the kth symbol of the ith user for $i=1,\ldots,NI$ and $k=0,\ldots,Q-1$. However, the projection $\mathbf{\Pi}_n$ in (32) is formed to be orthogonal to the signal subspace that spans contributions from the NI users. To avoid rejection of $s_n^{i,k}\underline{Y}_{k,n}^i$ as part of $\underline{I}_n$ and allow extraction of the desired signal component $\hat{s}_n^{i,k}$, we modify the projection $\mathbf{\Pi}_n$ and the combiner $\underline{W}_n^{i,k}$ as follows:

$$\mathbf{\Pi}_n^{i,k}=\mathbf{I}_{N_T}-\hat{\mathbf{C}}_n\mathbf{Q}_n\hat{\mathbf{C}}^{i,k^H}\tag{37}$$

$$\underline{W}_n^{i,k}=\frac{\mathbf{\Pi}_n^{i,k}\underline{\hat{Y}}_{k,n}^i}{\underline{\hat{Y}}_{k,n}^{i^H}\mathbf{\Pi}_n^{i,k}\underline{\hat{Y}}_{k,n}^i}\tag{38}$$

but still use the same single matrix inversion of (31) in $\mathbf{Q}_n$. The new projection $\mathbf{\Pi}_n^{i,k}$ specific now to ith user and its kth symbol uses an estimate of the signal blocking matrix $\hat{\mathbf{C}}^{i,k}$ defined in Table II. This matrix which spans $(\underline{I}_n-s_n^{i,k}\underline{Y}_{k,n}^i)$, and *a fortiori* $\underline{I}_{\mathrm{ISI},n}^{i,k}$ (i.e., $\underline{I}_{\mathrm{ISI},n}^{i,k}\in\mathrm{Vec}\{\hat{\mathbf{C}}^{i,k}\}$), avoids suppression of the desired signal and rejects ISI[12] along various ISR decompositions. In summary, the joint ISR combiner $\underline{W}_n^{i,k}$ now conforms to the constraints shown in (39) at the bottom of the page. Using the result $\underline{\hat{Y}}_{k,n}^{i^H}\mathbf{\Pi}_n^{i,k}\underline{\hat{Y}}_{k,n}^i=\underline{\hat{Y}}_{k,n}^{i^H}\underline{\hat{Y}}_{k,n}^i$ and the implicit definition of the MRC combiner in (28), we show that

[12]Next we exploit this useful property of joint ISR detection to explicitly address ISI rejection for the weak-power low-rate user treated earlier.

$$\begin{cases}\underline{W}_n^{i,k^H}\underline{Y}_{k,n}^i=1,\\ \underline{W}_n^{i,k^H}\mathbf{C}_n^{i,k^H}=0,\end{cases}\Rightarrow\begin{cases}\underline{W}_n^{i,k^H}\underline{Y}_{k,n}^i=1,\\ \underline{W}_n^{i,k^H}\left(\underline{I}_{\mathrm{ISI},n}^{i,k}+\sum_{\substack{i'=1\\ i'\neq i}}^{NI}\psi_n^{i'}\underline{Y}_n^{i'}\right)=0\end{cases}\tag{39}$$

$\underline{W}_n^{i,k} = \mathbf{\Pi}_n^{i,k}\underline{W}_{\mathrm{MRC},n}^{i,k}$. The ISR signal component estimate becomes

$$\begin{aligned}\hat{s}_n^{i,k} &= \underline{W}_n^{i,k^H}\underline{Y}_n = \underline{W}_{\mathrm{MRC},n}^{i,k^H}\left(\underline{Y}_n - \hat{\mathbf{C}}_n^{i,k}\mathbf{Q}_n\hat{\mathbf{C}}_n^H\underline{Y}_n\right)\\ &= \underline{W}_{\mathrm{MRC},n}^{i,k^H}\left(\underline{Y}_n - \hat{\mathbf{C}}_n^{i,k}\underline{v}_n\right)\\ &= \hat{s}_{\mathrm{MRC},n}^{i,k} - \underline{W}_{\mathrm{MRC},n}^{i,k^H}\hat{\mathbf{C}}_n^{i,k}\underline{v}_n \end{aligned} \tag{40}$$

where the $N_c\times 1$ vector $\underline{v}_n = \mathbf{Q}_n\hat{\mathbf{C}}_n^H\underline{Y}_n$ is common to all users and $\hat{s}_{\mathrm{MRC},n}^{i,k}$ is a new notation for the MRC signal component estimate of (28).

The soft outputs $\underline{v}_n$ of the *linearly-constrained* combiner[13] $\hat{\mathbf{C}}_n\mathbf{Q}_n$ [28] are actually estimates within a multiplicative factor of the parameters over which the interference is decomposed.[14] For a given ISR parametric decomposition, the interference to be suppressed $\underline{I}_n - s_n^{i,k}\underline{Y}_{k,n}^i$ is hence reconstructed as $\hat{\mathbf{C}}_n^{i,k}\underline{v}_n$ then subtracted from $\underline{Y}_n$ before MRC combining in (40). ISR can therefore be interpreted as a new *linearly-constrained* linear IC method. Indeed, the one-stage linear PIC [11], [13] resembles closely ISR-H when $M = 1$ antenna and when $\mathbf{Q}_n$ is set to the identity matrix (i.e., MRC combiner $\hat{\mathbf{C}}_n$). In contrast, ISR exploits soft outputs from a *linearly-constrained* combiner and thereby replaces error-sensitive subtraction by more robust nulling.

Note that the H mode can use $\mathrm{W}_n^{i,k} = \hat{\mathbf{C}}_n\mathbf{Q}_n\mathbf{I}_{N_T}^{(Q+2)*(i-1)+k+2}$ as an alternative direct implementation of the ISR combiner. Note also that the ISR DF modes require feedback of the current and future symbol estimates $\hat{b}_{nQ+k}$ for $k = 0,\ldots,Q$ which are derived in a preliminary stage from the MRC signal component estimates $\hat{s}_{\mathrm{MRC},n}^{i,k}$ for $k = 0,\ldots,Q$. Using the resulting ISR outputs to iterate the ISR process again gives rise to multistage ISR addressed in Section III-G.

D. Group/Hybrid Detection and ISI Rejection

The two generic cases of the mixed-rate and homogeneous-rate traffic scenarios addressed in Sections III-A and C, respectively, can be easily extended to group detection [14], [28], [29], [33] where ISR suppression is implemented among groups of users following a hierarchy in rate or power. A given group of users can suppress other selected interfering groups and possibly implement mutual suppression within that group by joint ISR detection, if required. Additionally, the ISR detector can implement hybrid modes of suppression (e.g., RH in Section III-B). Hybrid ISR is applicable to mixed rates where the duration QT includes different numbers of symbols for the respective interferer rates. It may also be used for mixed modulations where the decomposition is over different types of symbols. More generally, suppression modes may be mixed, some dimensions applying constraints from the D mode, others from the R mode, etc. One could design an optimal suppression strategy that would allocate the null constraints/modes among users and groups in the most efficient way to achieve the best performance/complexity tradeoff. However, this goes beyond the scope of this paper.

One can readily illustrate group and hybrid ISR by addressing ISI rejection for the weak-power low-rate user dealt with in the mixed-rate scenario of Section III-A. We consider that the dth user constitutes itself a group of Q virtual users, each virtual user being associated with a desired symbol to be extracted. The ensemble of these virtual users is characterized by $\underline{Y}_n^d$ in the observation space. The parametric decompositions of ISR apply to $\underline{Y}_n^d$. They give rise to the constraint matrix $\mathbf{C}_n^d$ indexed with d and the corresponding blocking matrix $\mathbf{C}_n^{d,k}$ for the kth virtual user (or symbol) along any of the ISR modes described (e.g., $\mathbf{C}_n^d = [\underline{Y}_n^d]$ and $\mathbf{C}_n^{d,k} = [\underline{I}_{\mathrm{ISI},n}^{d,k}]$ in the TR mode). Note that hybrid ISR constructs $\hat{\mathbf{C}}_n^d$ for the dth user and $\hat{\mathbf{C}}_n$ for the NI interfering users along different modes.

The ISR combiner that extracts the kth symbol of the dth user is therefore updated to reject ISI by incorporating joint ISR among the Q desired symbols in (31) to (33) as follows:

$$\bar{\mathbf{C}}_n^d = \mathbf{\Pi}_n\hat{\mathbf{C}}_n^d \tag{41}$$

$$\bar{\mathbf{C}}_n^{d,k} = \mathbf{\Pi}_n\hat{\mathbf{C}}_n^{d,k} \tag{42}$$

$$\mathbf{Q}_n^d = \left(\bar{\mathbf{C}}_n^{d^H}\bar{\mathbf{C}}_n^d\right)^{-1} \tag{43}$$

$$\mathbf{\Pi}_n^{d,k} = \mathbf{I}_{N_T} - \bar{\mathbf{C}}_n^d\mathbf{Q}_n^d\bar{\mathbf{C}}_n^{d,k^H} \tag{44}$$

$$\bar{\mathbf{\Pi}}_n^{d,k} = \mathbf{\Pi}_n^{d,k}\mathbf{\Pi}_n \tag{45}$$

$$\underline{W}_n^{d,k} = \frac{\bar{\mathbf{\Pi}}_n^{d,k}\hat{\underline{Y}}_{k,n}^d}{\hat{\underline{Y}}_{k,n}^{d^H}\bar{\mathbf{\Pi}}_n^{d,k}\hat{\underline{Y}}_{k,n}^d}. \tag{46}$$

Both $\mathbf{Q}_n$ and $\mathbf{\Pi}_n$ still use (31) and (32). Notice that if there are no strong interferers to be suppressed, we may still reject ISI before despreading by setting $\mathbf{\Pi}_n$ to the identity matrix. If we also replace $\mathbf{\Pi}_n^d$ by the identity matrix, then we revert to a simple MRC combiner.

ISR offers a unifying framework that approaches IC methods at the low end (i.e., TR) and the ZF decorrelator-type receivers at the high end (i.e., H&D). Its general formulation can reduce to simple MRC above and it can also be extended to MMSE-type criteria in the next section.

E. Weighted ISR and Centralized Versus Blind Structures

An additional remedy to noise enhancement addressed in Sections III-A and B is to relax the null constraints and assign a penalty weight to noise amplification in the ISR suppression process. This variant of ISR, referred to as weighted ISR, modifies the general ISR combiner solution of (31) to (33) as follows:

$$\bar{\mathbf{C}}_n = \hat{\mathbf{C}}_n\mathbf{\Lambda}_n \tag{47}$$

$$\bar{\mathbf{Q}}_n = \left(\bar{\mathbf{C}}_n^H\bar{\mathbf{C}}_n + \lambda\mathbf{I}_{N_c}\right)^{-1} \tag{48}$$

$$\mathbf{\Pi}_n = \mathbf{I}_{M*(2L-1)} - \bar{\mathbf{C}}_n\bar{\mathbf{Q}}_n\bar{\mathbf{C}}_n^H \tag{49}$$

$$\underline{W}_n^{d,k} = \frac{\mathbf{\Pi}_n\underline{Y}_{k,n}^d}{\underline{Y}_{k,n}^{d^H}\mathbf{\Pi}_n\underline{Y}_{k,n}^d} \tag{50}$$

where $\mathbf{\Lambda}_n$ is an $N_c\times N_c$ diagonal matrix of positive weights and λ an additional weighting factor.

[13]The jth column of the combiner $\hat{\mathbf{C}}_n\mathbf{Q}_n$ has a unit response to the jth column of $\hat{\mathbf{C}}_n$ and null responses to its other columns.

[14]In the D mode for instance, the generic term of $\underline{v}_n$ is proportional to $\psi_n^i\zeta_{f,n}^i$. This feature enables a cost-effective joint detection and channel estimation scheme in one step [17].

One can show that the above general weighted ISR solution reduces to MMSE combining with respect to the ISR signal decomposition selected by setting $\lambda = \hat{\sigma}_N^2$, the noise variance estimate, and

$$\mathbf{\Lambda}_n = \begin{cases} [1], & \text{in the TR mode} \\ \left[\ldots, \hat{\psi}_n^i, \ldots\right], & \text{in the R mode} \\ \left[\ldots, \hat{\psi}_n^i \left|\hat{\zeta}_{f,n}^i\right|, \ldots\right], & \text{in the D mode} \\ \left[\ldots, \underbrace{\hat{\psi}_n^i, \ldots, \hat{\psi}_n^i}_{(Q+2)\text{ times}}, \ldots,\right], & \text{in the H mode.} \end{cases} \tag{51}$$

The instantaneous parameter estimates in the equation above can be further averaged or smoothed in time. The columns of the constraint matrix estimate $\hat{\mathbf{C}}_n$ are reconstructed without normalization. For lack of space, this version of weighted ISR referred to as MMSE-ISR will not be pursued and will be addressed in a future work.

Note however that weighted ISR extends the unifying framework of ISR suppression by approaching centralized MMSE multiuser receivers [9], [10], [34]–[36] at the high end (i.e., MMSE ISR-H and D) and weighted IC methods [37] at the low end (i.e., MMSE ISR-TR). In fact, weighting in IC methods is applied to data decisions instead of noise [37]. In this regard, we developed another version of ISR that introduces weights over data decisions reflecting our confidence in those decisions. For lack of space, we refer the reader to [38] for more details about this variant of ISR referred to as partial ISR.

Note also that the above versions of ISR still assume that the noise vector is uncorrelated both in space and time. They would optimally require knowledge of the codes of all users to process them all. Non-centralized MMSE receivers such as [39], [40] attempt to optimally suppress all users without knowledge of their codes. Yet our experience is that the centralized receivers are more robust to time-variations than the noncentralized or blind versions [28], [29]. In this regard, the noncentralized receivers require use of short codes [39], [40] to enable tracking of cyclo-stationary signals. Nevertheless, operation without knowledge of the user codes remains an advantage for these receivers.

Regarding this issue, ISR indeed requires knowledge of interferers' codes, but only those of a few high-power high-rate users in the served cell due to complexity limitation. These codes are readily available at the base station on the up-link. On the downlink, we envisage use of Walsh codes [18], [19] *a priori* known to the mobile. Overall, the computational power available should allow implementation of ISR on either link with a centralized suppression limited to a few high-power high-rate users. Other high-power high-rate users can be suppressed blindly by combining ISR, MMSE-ISR or partial ISR (or all together) with the partially-centralized hybrid ZF/blind MMSE scheme in [29]. This *ad hoc* extension will be detailed in a future work.

F. Successive Versus Parallel Detection

It is already documented in literature that successive IC may sometimes outperform parallel IC. For instance, SIC and PIC are compared to conclude that SIC outperforms PIC in adverse power control situations, whereas PIC outperforms SIC when power control is perfect [41], [42]. Also the decorrelating decision feedback algorithm [14] uses a successive structure. In a first stage, the signal is whitened, then DF is used successively in the second stage, processing in order of decreasing strengths. Although this presentation of ISR has been focused on a parallel implementation, ISR may also be implemented in a successive manner, denoted ISR-S in what follows.

Without loss of generality, let us consider the operation of ISR-S among the NI users sorted in order of decreasing strength such that user $i = 1$ is the strongest and user $i = NI$ is the weakest. The ISR-S signal component estimate for the kth symbol of the ith user is, hence, given by

$$\begin{cases} \underline{v}_{i,n} = \mathbf{Q}_{i,n}\hat{\mathbf{C}}_{i,n}^H \underline{Y}_n, \\ \hat{s}_n^{i,k} = \hat{s}_{\mathrm{MRC},n}^{i,k} - \underline{W}_{\mathrm{MRC},n}^{i,k^H}\hat{\mathbf{C}}_{i,n}^{i,k}\underline{v}_{i,n} \end{cases} \tag{52}$$

where $\hat{\mathbf{C}}_{i,n}$ spans only the subspace of users $1, \ldots, i-1$ (and also of user i if ISI rejection is desired), and $\hat{\mathbf{C}}_{i,n}^{i,k}$ denotes the corresponding signal blocking matrix. Clearly, $\hat{\mathbf{C}}_{i,n}$ is no longer common to all users, which requires the expensive matrix inversion to be performed for each user. However, this inversion is avoided with ISR-TR since $\mathbf{Q}_{i,n} = (\hat{\mathbf{C}}_{i,n}^H \hat{\mathbf{C}}_{i,n})^{-1}$ is a scalar. ISR-TR-S represents an alternative to its parallel counterpart, ISR-TR, and provides an ISR analog to SIC. Other modes may take advantage of the common elements of $\hat{\mathbf{C}}_{i,n}$ from one processing cycle to the next using matrix inversion by partitioning [43], although this has not been considered. The disadvantage of ISR-S is the long processing delay. It may be useful to consider the tradeoffs between parallel processing and serial processing similar to the hybrid interference canceller (HIC) [44], [45] which combines the often better performance of SIC with the parallel structure of PIC.

G. Multistage Processing: M-Option

The DF modes of ISR (i.e., TR, R, and D) use coarse MRC symbol estimates at a preliminary stage in order to reconstruct signals for the ISR operation (see Section III-C). MRC estimates are less reliable than ISR estimates causing worse reconstruction errors. We may use improved ISR estimates to reconstruct and perform the ISR operation again in successive stages to provide better results [11]. This multistage approach illustrated in Fig. 2 and referred to as the M-option processes the signal component estimate for the kth symbol, $k = 0, \ldots, Q-1$, of the ith user in N_s stages[15] as shown in (53) at the bottom of the next page where $\hat{s}_n^{i,k}(1)$ is the signal component estimate from first ISR stage and $\hat{\mathbf{C}}_n(0), \hat{\mathbf{C}}_n^{i,k}(0), \hat{\mathbf{Q}}_n(0), \underline{v}_n(0)$ are formed from symbol estimates at the preliminary stage (i.e., $\hat{b}_{nQ+k}^i(0) \leftarrow \hat{s}_n^{i,k}(0)$). Iterating the process,[16] we find the signal component and symbol estimates at stage N_s (i.e., $\hat{s}_n^{i,k} = \hat{s}_n^{i,k}(N_s) \rightarrow \hat{b}_{nQ+k}^i$).

[15]One stage means that the ISR operation is performed only once. Strictly speaking, it is a two-stage approach with a conventional MRC preliminary stage (see Fig. 2).

[16]Note that intermediate frame channel-decoding can be combined with multistage ISR [22] for further improved performance.

The multistage approach has a cost in increased complexity; however, complexity can be reduced because many computations from one stage to the next are redundant. For example, the costly computation of $\underline{v}_n(j)$ could be tracked instead, because $\underline{v}_n(j) \approx \underline{v}_n(j-1)$ if the symbol estimation errors do not change much from stage to stage, which can be expected in most situations.

Application of the M-option to PIC follows the same approach. The M-option may also be generalized to the successive structures ISR-S and SIC. For ISR-TR-SM the approach is as follows: The first stage is as usual, but the following stages take advantage of reconstructed interference available from the previous stage. When user i is processed at stage i, users $i+1,\ldots,NI$ are reconstructed from the estimated symbols of stage $i-1$; whereas users $1,\ldots,i-1$ are reconstructed from previous estimates of the same stage. Except for the first stage, ISR-TR-SM therefore also nulls lower power users. The same approach is used for SIC-M.

IV. Discussion of ISR Advantages

A. Interference Rejection Paradigm

Multiuser detection techniques differ in the way they characterize interference and in the way they suppress it. Like IC methods [11]–[13] at the low end in complexity, ISR characterizes interference by its signal contribution $\underline{I}_n$ to the observation vector $\underline{Y}_n$. ISR-TR and ISR-TRS, the closest to PIC [11], [12] and SIC [12], [13], respectively, reconstruct this contribution $\hat{\underline{I}}_n$ then suppress it. However, unlike IC techniques, ISR replaces error-sensitive subtraction by more robust nulling[17] to estimation errors and can be interpreted as a new *linearly-constrained* IC method (see Section III-C). Linear IC methods [47], [48] also replace nonlinear hard decision by linear soft-decision feedback and result into a cascade[18] of projectors [47], [48]. However, ISR exploits soft outputs from a linearly constrained combiner and thereby implements more robust nulling of interference along various interference subspace decompositions (or characterizations).

Madkour *et al.* characterized the interference by subspaces similar in span to those used in the TR and R modes with one antenna in [18] and [19], respectively, then suppressed this interference by projections. Unlike ISR, however (see Section IV-B), they implemented signal combining over the cleaned observation with a RAKE-type receiver. Our work, carried out independently, provides a framework for interference subspace rejection that stems from various parametric decompositions of the interference. These decompositions are motivated by the resulting improved robustness to errors in power control, channel parameter estimation, and symbol decisions. They provide a more complete understanding of the performance/complexity tradeoffs available. Overall, ISR offers much more extended applicability (see options and applications in Section III).

At the high end in complexity, the decorrelator [6]–[8] and the ZF-DF partial decorrelator [14] can be regarded as a combination of the H and D modes of ISR with one antenna. This hybrid of ISR is also similar to the projection receiver (PR) [50], [51], which implements a ZF-type detector through exploitation of a projector orthogonal to the interference subspace. In the general case, however, ISR characterizes interference from different interference subspace decompositions and accordingly suppresses it along modes (i.e., TR, R, D, H, etc...) that require reduced complexity. Computational power is what limits exploitation of ISR-H today, and *a fortiori* the more complex decorrelator-type receivers. Other ISR modes require tolerable complexity and offer significant gains over IC detectors (see Section V).

B. Signal Combining

Note that the observation model of (26) merges space and time into a vector dimension and therefore allows joint combining over multipaths and antennas in one step.[19] Multiuser combining in [34], [52] also matches a composite channel over multipaths, but unlike STAR [15] it uses one antenna and "nonparametric" channel estimation. To our knowledge, the advantages of simultaneous matched combining and interference suppression were not recognized previously and were not pursued to further integrate the spatial dimension made available by antenna arrays. Tsatsanis and Giannakis [35] simply commented on possible extension of their multirate filter model of CDMA access to spatial sampling using multiple antennas. Paulraj and Papadias [53] developed a more general model for multiple access techniques but resorted to 2D-RAKE receiver solutions that separate processing in space and time in the CDMA case. Current CDMA solutions similarly propose multiuser processing post-combining [54], [55] or precombining [36], [55], [56] over multipaths and/or antennas in a RAKE-like receiver structure. The post-combining solutions do not exploit multiuser detection capabilities to improve channel estimation [36]. Thereby both signal combining and interference suppression can be degraded. The precombining approaches do not exploit the advantages of diversity and process fingers individually as if they were

[17]Advantages of interference suppression by nulling with projections instead of subtraction were previously recognized in an acoustic echo cancellation application in [46].

[18]Although linear IC approaches the decorrelator [47], [48], it performs worse than nonlinear IC in selective fading [34], [49] .

[19]This feature is inherited from the post-correlation model [15] for which an ISR version over despread signals is available.

$$\begin{cases} \hat{s}_n^{i,k}(0) = \hat{s}_{\mathrm{MRC},n}^{i,k} & \longrightarrow \left\{\hat{\mathbf{C}}_n(0), \hat{\mathbf{C}}_n^{i,k}(0), \hat{\mathbf{Q}}_n(0), \underline{v}_n(0)\right\} \\ \hat{s}_n^{i,k}(1) = \hat{s}_{\mathrm{MRC},n}^{i,k} - \underline{W}_{\mathrm{MRC},n}^{i,k^H} \hat{\mathbf{C}}_n^{i,k}(0)\underline{v}_n(0) & \longrightarrow \left\{\hat{\mathbf{C}}_n(1), \hat{\mathbf{C}}_n^{i,k}(1), \hat{\mathbf{Q}}_n(1), \underline{v}_n(1)\right\} \\ \quad\vdots & \vdots \\ \hat{s}_n^{i,k}(N_s) = \hat{s}_{\mathrm{MRC},n}^{i,k} - \underline{W}_{\mathrm{MRC},n}^{i,k^H} \hat{\mathbf{C}}_n^{i,k}(N_s-1)\underline{v}_n(N_s-1) & \longrightarrow \hat{s}_n^{i,k} = \hat{s}_n^{i,k}(N_s) \end{cases} \tag{53}$$

separate users with fractioned power [54], [49]. Complexity is thereby increased as if more users were to be processed while depriving multiuser detection of the diversity advantages. Unlike previous methods, STAR-ISR fully exploits both space and time diversities as well as the array-processing potential offered by the antennas while carrying out simultaneous channel and timing estimation [15], [30], signal combining and inherent interference rejection.

C. The Edge Effect and ISI

The edge effect and ISI relate to the difficulties introduced by the symbols at the edges of the processed frames and those surrounding the desired symbol. They arise in asynchronous transmissions from the self-ISI vector $\underline{I}_{\mathrm{ISI},n}^{d,k}$ and similarly from the multiple-access (MA-ISI) vectors $\underline{I}_{\mathrm{ISI},n}^{i,k}$. DF methods [11]–[14] rely on error-sensitive one-shot hard decision and feedback to remove the edge effect. Linear receivers resort to long sequence estimation and thereby reduce the edge effect to a negligible amount [4]. The edge effect is completely suppressed in [58] by subtraction. Future symbols are predicted there using convolutional coding. Simpler methods eliminate the edge effect by transmitting bursts of symbols or by inserting isolation bits [57]. ISR effectively isolates the current symbol without reducing the transmission-rate and treats the equally-isolated adjacent symbols as virtual interferers (see Section III-D). Near–far resistant nulling in ISR removes MA-ISI interference while self-ISI is simply suppressed by dedicated null-constraints (see Sections III-C and D). In both the single-symbol-based (i.e., $Q = 1$) and block estimation cases, this approach does not suffer from the edge effect. It holds over a large observation window of symbols that allows treatment of wider interpath and interuser delay spreads as well as permits *ad hoc* extension to multirate detection.

D. Unifying Framework and Extended Applicability

ISR offers a unifying framework for multiuser detection that reaches IC detectors and linear receivers at both ends in performance and complexity. It can be interpreted as a new *linearly-constrained* linear IC method and can be adapted to implement MMSE-type criteria and/or weighting over symbol decisions in partial ISR [38]. It applies to completely asynchronous transmissions, to one-shot or block estimation, and to multimodulation, multirate, or even multicode CDMA. ISR can be adapted to the downlink and to MIMO systems [22] and efficiently combines with channel identification with STAR [30]. Overall, it offers an efficient and cost-effective multiuser receiver solution for wideband CDMA.

V. Simulations and Discussion

In this section, we provide simulation results that compare ISR modes with SIC and PIC. We summarize these results and discuss application of the modes.

A. Simulation Setup

In the simulations that follow, we attempted to approximate the specifications for up-link WCDMA [2] in a homogeneous-rate scenario. We consider a differentially encoded BPSK DS-CDMA with NI in-cell users sharing the channel; whereas out-of-cell users along with thermal noise are modeled as additive white Gaussian noise (AWGN). For lack of space, we refer the reader to [16] where we report on a mixed-rate traffic situation that mixes BPSK and 8-PSK users, a scenario currently studied in new wireless technologies such as EDGE or OFDM for high-speed wireless data access [59]. The channel is considered Rayleigh fading [60] with chip normalized Doppler $f_D T_c$, and we consider frequency-selective fading with $P = 3$ propagation paths. Transmitters are equipped with one transmit antenna; whereas the receiving end is equipped with $M = 1$ or 2 antennas. We implement closed-loop power control, with a power control correction factor ΔP_{PC} to be updated and adjusted every 2560 chips with a simulated transmission delay of 0.625 ms and an error rate on the power control bit of $\mathrm{BER}_{PC} = 10\%$.[20] The parameters most commonly utilized in the simulations, unless otherwise is specified, are listed in Table III. STAR [15] is used to estimate temporal delays and channel gain, except for ISR-D which uses its own estimator (see footnote 14). Thus the capacity figures obtained for STAR-PIC/SIC are significantly higher than those obtainable with RAKE-PIC/SIC. For lack of space, only single-symbol-based estimation ISR (i.e., $Q = 1$) is studied.

TABLE III
Parameters Used in Simulations (Unless Otherwise Specified)

Parameter	Value	Comment
R_c	4.096 Mcps	chip rate
M	1 or 2	number of antennas
P	3 (0 dB, -6 dB, -10 dB)	number of paths (relative average strength)
f_c	1.9 GHz	carrier frequency
f_D	8.9 Hz	Doppler frequency (*i.e.*, 5 Kmph)
f_e	300 Hz	offset error over f_c (uniform)
L	16	processing gain
f_{PC}	1600 Hz	frequency of PC updating
ΔP_{PC}	$\pm$0.5 dB	PC adjustment
BER_{PC}	10%	simulated PC bit error rate
$\frac{\delta\tau}{\delta t}T_c$	2 ppm	symbol clock drift (linear)
$\Delta\tau$	8 chips	maximal delay spread

B. Simulation Results

In Fig. 3, we show simulation results along with bit error rate (BER) bounds[21] for a system supporting $NI = 8$ users with processing gain $L = 16$ and other parameters as specified in Table III. With $L = 16$, the symbol rate is 256 kb/s and corresponds to 128 kb/s with simple 1/2 rate channel coding and decoding. ISR-D, DX(256) where 256 is the temporal dimension[22] is shown in Fig. 3(a), ISR-R,RX(256) in Fig. 3(b), ISR-TR,TRX(256) in Fig. 3(c), and ISR-H in Fig. 3(d). Completely

[20]Fixed to this value regardless of the actual channel BER.

[21]We have been able to derive accurate noise amplification factors due to ISR constraints and theoretical BER bounds in the asynchronous transmission case. For lack of space, we will report on these new analysis results in a future publication.

[22]Temporal dimension is $2L = 32$ for basic ISR (i.e., $Q = 1$ and $N_X = 0$).

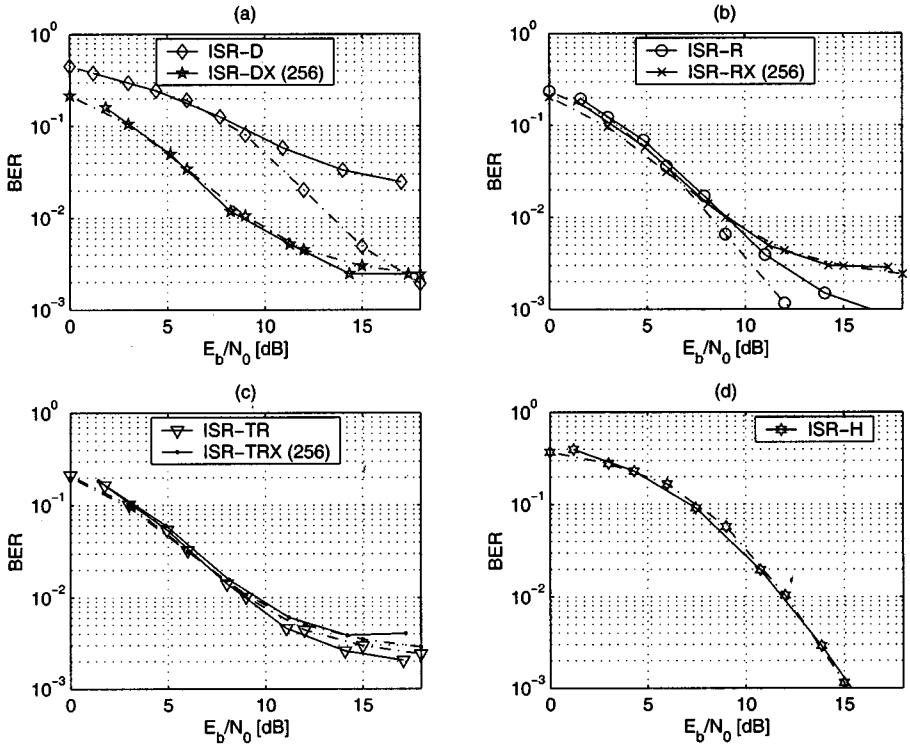

Fig. 3. BER versus E_b/N_0 performance of ISR with and without past data extension (X-option) for 8 DBPSK mobiles at 256 kb/s: simulated (solid) and lower bound (dashed). (a): ISR-D,DX. (b): ISR-R,RX. (c): ISR-TR,TRX. (d): ISR-H.

asynchronous transmission was considered with the X-option while quasisynchronism was used otherwise.[23] Bounds are extremely tight at low to moderate SNR and differences appear only at high SNR when identification errors become dominant. The X-option is seen to be very effective with ISR-D and has only little effect on ISR-TR and ISR-R. We note again that the DF modes flatten at high SNR indicating that the DF modes have zero asymptotic efficiency. ISR-H provides some asymptotic efficiency, but has very poor performance at low to moderate SNR.

In later simulations we focus on a BER of 5% which is considered applicable to WCDMA [1], [2] before channel decoding. The general picture is that ISR-H performs poorly compared to the other modes in this range and therefore is not considered further. ISR-H proves valuable in mixed power or modulation [16]. To support completely asynchronous transmission, the X-option is used by default in what follows.

Fig. 4 depicts the E_b/N_0 required to obtain a BER of 5% for increasing number of users NI, as obtained by searching around the target BER. The figure shows also performance of ISR-TRX-S, SIC, and PIC. The system setup is the same as previous section. All DF ISR modes provide roughly the same capacity ($NI \leq 14$), but higher than subtractive receivers, particularly when the system load is high. The successive implementation of ISR-TRX, ISR-TRX-S, provides slightly worse performance than its parallel version, but better than SIC. ISR-TRX-S and SIC are similar up to the point of interference rejection; ISR-TRX-S nulls interference, whereas SIC subtracts it. ISR-TRX-S therefore gains robustness compared to SIC by virtue of its higher robustness to estimation errors and especially to power estimation errors.

[23]Simply because the X-option enables complete asynchronous support as discussed in Section III-B.

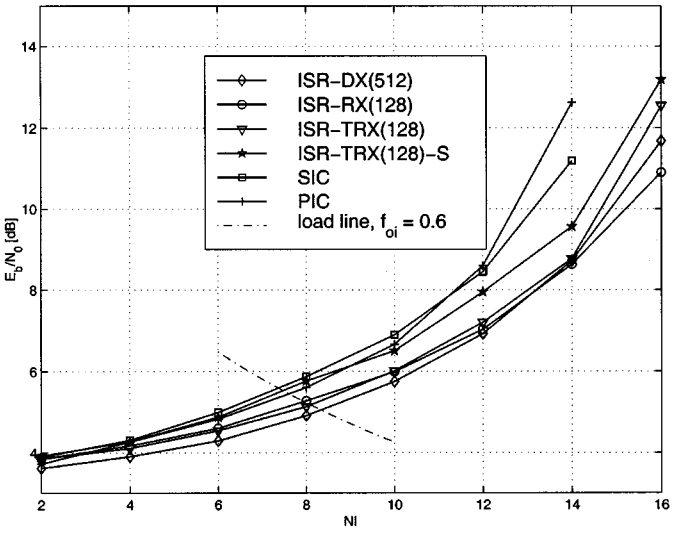

Fig. 4. Required E_b/N_0 at 5% BER before FEC decoding versus the system load NI in DBPSK mobiles at 256 kb/s: single-antenna case.

The load line dictates the operating condition when all in-cell but not out-cell interference is suppressed, while neighboring cells are assumed to have same load as the target cell and when the out-cell to in-cell interference ratio is $f_{\mathrm{oi}} = 0.6$ [20]. Capacity ranges from 7.5 users (SIC) to 8.5 users (ISR-D). These capacities may be exceeded if out-cell interferers are suppressed as well, or if the cell is isolated.

1) Multiple Antennas: Fig. 5 shows performance with $M = 2$ antennas. Generally speaking, all methods gain performance

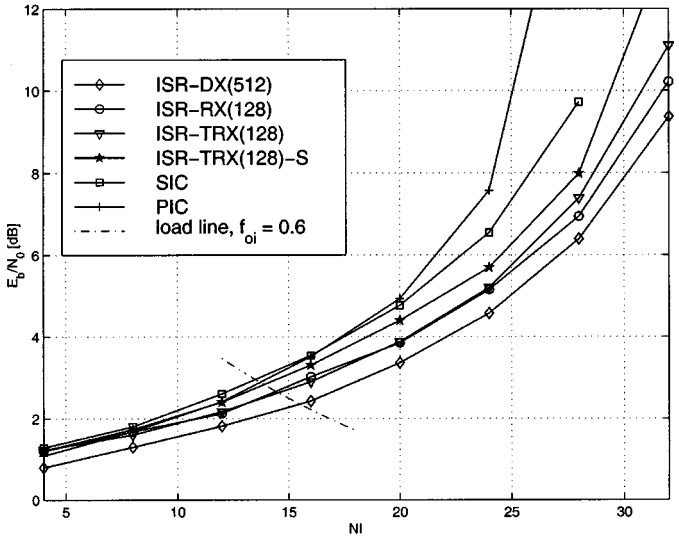

Fig. 5. Required E_b/N_0 at 5% BER before FEC decoding versus the system load NI in DBPSK mobiles at 256 kb/s: two-antenna case.

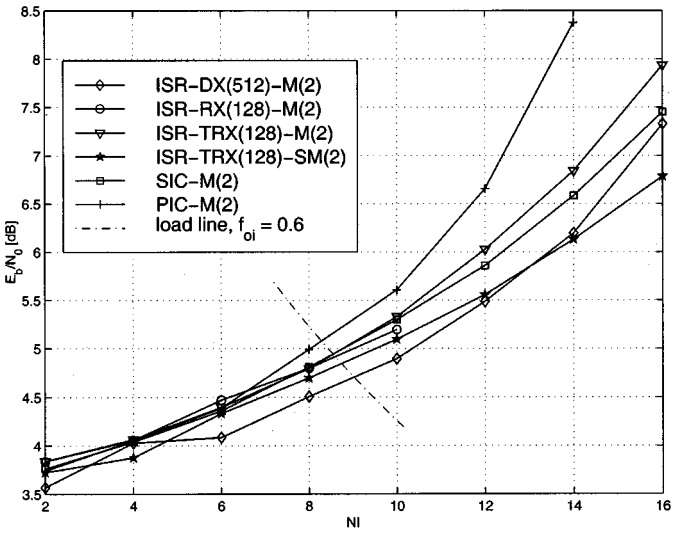

Fig. 6. Required E_b/N_0 at 5% BER before FEC decoding versus the system load NI in DBPSK mobiles at 256 kb/s: two-stage multistage ISR processing case.

by the same amount. Required SNR is about 3 dB lower and the number of users accommodated is doubled. This increase is not surprising, since the noise is now distributed over two receiving antennas and the dimensionality is doubled. Furthermore, variations in total received power are reduced because the number of diversities $N_f = MP$ is doubled. ISR-D offers slightly better performance than other DF modes (less than 0.5 dB) because the E_b/N_0 operating point is generally 3 dB lower, which degrades channel identification. This tends to favor ISR-D which is completely insensitive to estimation errors of the channel gain. Again, ISR-TRX-S outperforms its nonlinear companion SIC. The load line suggests that at the low end 13.5 users can be supported with PIC but ISR-DX may serve about 15.5 users. Doubling the number of antennas, therefore, increases capacity by about 1.8.

2) Multistage Processing: M-Option: Fig. 6 provides performance curves with one antenna when the number of ISR stages is increased to two. Comparing these to the one-stage curves of Fig. 4, the performance of all modes is improved by about 0.5 dB near $NI = 8$. This improvement increases to 5 dB for ISR-TRX at $NI = 16$. This confirms that DF based on MRC estimates for one-stage operation is good when interference noise is low (low or moderate number of users), but becomes degraded at high degree of interference (high NI). SIC-M and ISR-TRX-SM achieve performance comparable to DF ISR-M modes, but not ISR-DX-M. However, ISR-TRX-SM is better than SIC-M with performance close to ISR-DX-M and even relatively better at very high loads. ISR-TRX-SM is a very attractive solution for high performance. It suffers, however, from an increase in processing delay.

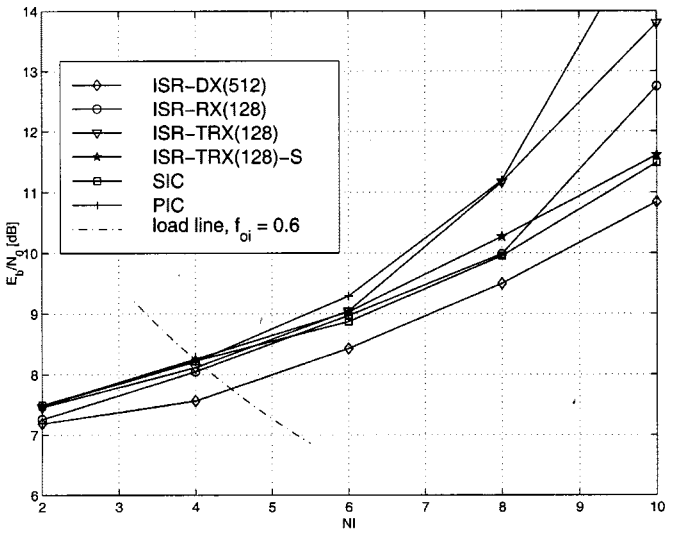

Fig. 7. Required E_b/N_0 at 5% BER before FEC decoding versus the system load NI in DBPSK mobiles at 256 kb/s: high-Doppler case (i.e., 100 kmi/h).

3) High Doppler: In Fig. 7, we have increased the Doppler by a factor of 20 reflecting mobile speeds of 100 Kmph. All modes of operation suffer from increased Doppler because power control is not able to follow the variations of the channel, causing greater power fluctuations and worse identification of the channel. Again, this is seen to favor ISR-DX (relative to other modes) which promises the best robustness to channel identification errors. As expected, ISR-RX suffers more than ISR-DX but ISR-TRX suffers the most as it is the least robust DF mode. Large variations in power are seen to favor the successive methods. SIC and ISR-TRX-S have same performance and outperform ISR-TRX,RX but not ISR-DX. PIC and ISR-TRX have poor performance in high Doppler. Capacity is reduced to 4 (PIC) and 4.5 (ISR-DX) as seen from the load line, a reduction by a factor of almost 2. Fortunately, practical systems are dominated by users with low mobility and, therefore, this reduction may not be important in practice.

C. Discussion

Generally, all ISR modes of operation with DF outperform receivers with interference cancellation by subtraction (SIC and PIC). Only in high Doppler and multistage is SIC able to take sufficient advantage of successive processing of users to outperform ISR-TRX,RX; but not ISR-DX. However, the ISR alternative to SIC, ISR-TRX-S provides mostly better

TABLE IV
PERFORMANCE FEATURES AND COMPLEXITIES OF SINGLE-SYMBOL-BASED ESTIMATION (i.e., $Q = 1$) ISR MODES WITH STAR

				Robustness to estimation errors of				
—	IC method	N_c	Delay †	Timing	Phase	Power	Symbols	Complexity [Gops]‡ $NI = 8/16/32$
PIC	subtracts reconstructed interference	—	1+1PC					2.2/4.2/8.4
SIC	subtracts reconstructed interference of higher power users	—	1+NIPC					2.2/4.2/8.4
ISR-H	nulls reconstructed bits of interfering users	$3NI$	1PC		✓	✓	✓	13.9/52.0/220.6
ISR-DX	nulls reconstructed interfering diversities	$N_f NI$	1+1PC		✓	✓		8.3/27.4/102.9
ISR-RX	nulls reconstructed interfering users	NI	1+1PC		(some)	✓		4.7/13.8/45.7
ISR-TRX	nulls total reconstructed interference	1	1+1PC			(some)		2.2/4.2/8.4
ISR-TRX-S	nulls total reconstructed interference of higher power users	1	1+NIPC			(some)		2.2/4.2/8.4
ISR-TRX-M(2)	nulls total ISR reconstructed interference	1	1+2PC			(some)	(some)	2.9/5.5/11.0*

†Refers to a user with processing gain 256. For smaller processing gains it ranges from 1+1PC to 256/L+1PC. It can, however, always be reduced to 1+1PC considering smaller observation windows at a cost of increased complexity.

‡Based on an observation length $N_T = 512$ chips (section III-B), chip rate 4.096 Mcps, $M = 1$ antenna, $P = 3$ paths and provided as a total over NI users and includes STAR. Note that ISR-H requires the same number of constraints as ISR-D; however, ISR-D has real-valued constraints which lower its complexity. Actual processing gain of users has negligible impact on complexity.

* This complexity depends on the number of MRC symbol errors in preliminary stage relative to ISR symbol errors after first stage. It is assumed that the total complexity of ISR does not increase by more than 50%.

performance, underlining the strength of constrained subspace suppression rather than interference subtraction. ISR-TRX-S has same complexity as SIC and therefore is an attractive ISR solution for successive processing.

The complexity of the ISR techniques is mainly determined by the number of users to be cancelled and to a lesser extent by the number of users processed. The complexity differences arise mainly from differences in dimension of the matrix to be inverted in (31), which corresponds to the total number of constraints N_c imposed by the mode. A rough calculation is provided in Table IV along with the performance features of the ISR modes. The DF modes rank in performance as ISR-DX $>$ ISR-RX $>$ ISR-TRX, consistent with the exact ranking of complexity. Significant differences appear only in adverse situations such as high Doppler. ISR-TRX with complexity of the order of the PIC is, therefore, a very attractive solution in most situations as it combines affordable complexity with satisfactory performance. Further improvements in performance may be obtained at the least cost in complexity by increasing the number of processing stages. More precise estimation of one constraint by decreasing the data estimation errors yields better results than introducing modes with additional constraints. The strength of more elaborate modes such as ISR-H is to be found in adverse near–far situations [22], [30] or when identification of the channel is poor. This indication of theory is supported by simulations. However, as performance improves from one mode to another, the complexity required increases while the resulting SNR advantage decreases, making the last decibel of gain even more expensive to obtain.

VI. CONCLUSION

A new multiuser receiver structure, ISR, has been presented that offers a number of implementation modes covering a large range in performance and complexity. The low sensitivity to variations in interference power enables simultaneous support of both high-power high-rate and low-power low-rate transmissions in integrated multiservice wideband CDMA networks. ISR-H manifests the best performance but is the most complex to implement. ISR-TR may be the short-term preferred choice with respect to performance/complexity tradeoffs.

ISR-TRX provides generally very good performance in most situations when identification is good. Moreover, it always outperforms PIC and generally outperforms SIC, both of which possess the same level of complexity. ISR-TRX is therefore a very attractive solution for multiuser detection. Eventually, the evolution of DSPs, which tend to double in performance every one and a half years, may gradually allow for cost-effective implementation of ISR-RX,DX to achieve better performance. ISR-TRX-S represents an alternative to SIC, achieving better performance than SIC in all situations while requiring about the

same complexity. ISR-H was found to provide inferior performance for high data rates in the operating region of interest. However, its advantages were demonstrated in adverse near–far situations [16]. ISR-H is studied further in [30] with emphasis on downlink applications.

The tolerable complexity is best exploited by limiting the number of high-power users to that which the base station receiver can suppress and allowing as many low-power users as the SNR limit permits. Since overall complexity varies roughly linearly with the number of interferers suppressed, advances in tolerable complexity appear to be readily translatable to higher bandwidth efficiencies.

ACKNOWLEDGMENT

The authors would like to thank R. Matyas, L. Strawczynski, D. Bevan, and C. Ward of Nortel Networks for fruitful discussions which brought an interesting industrial perspective to this research work.

REFERENCES

[1] F. Adachi, M. Sawahashi, and H. Suda, "Wideband DS-CDMA for next generation mobile communications systems," *IEEE Commun. Mag.*, vol. 36, pp. 55–69, Sept. 1998.

[2] R. Prasad, "An overview of CDMA evolution toward wideband CDMA," *IEEE Commun. Surveys*, vol. 1, pp. 2–29, fourth quarter 1998.

[3] A. Duel-Hallen, J. Holtzman, and Z. Zvonar, "Multiuser detection for CDMA systems," *IEEE Pers. Commun.*, pp. 46–58, Apr. 1995.

[4] S. Moshavi, "Multiuser detection for DS-CDMA communications," *IEEE Commun. Mag.*, vol. 34, pp. 124–136, Oct. 1996.

[5] S. Verdu, "Minimum probability of error for asynchronous Gaussian multiple-access channels," *IEEE Trans. Inform. Theory*, vol. 32, pp. 85–96, Jan. 1986.

[6] K. S. Schneider, "Optimum detection of code division multiplexed signals," *IEEE Trans. Aerosp. Electron. Syst.*, vol. 15, pp. 181–185, Jan. 1979.

[7] R. Lupas and S. Verdu, "Linear multiuser detectors for synchronous code-division multiple-access channels," *IEEE Trans. Inform. Theory*, vol. 35, pp. 123–136, Jan. 1989.

[8] ——, "Near–far resistance of multiuser detectors in asynchronous channels," *IEEE Trans. Commun.*, vol. 38, pp. 496–508, Apr. 1990.

[9] Z. Xie, R. T. Short, and C. K. Rushforth, "A family of suboptimum detectors for coherent multiuser communications," *IEEE J. Select. Areas Commun.*, vol. 8, pp. 683–690, May 1990.

[10] U. Madhow and M. Honig, "MMSE interference suppression for direct-sequence spread-spectrum CDMA," *IEEE Trans. Commun.*, vol. 42, pp. 3178–3188, Dec. 1994.

[11] M. K. Varanasi and B. Aazhang, "Multistage detection in asynchronous code-division multiple-access communications," *IEEE Trans. Commun.*, vol. 38, pp. 509–519, Apr. 1990.

[12] R. Kohno, H. Imai, M. Hatori, and S. Pasupathy, "Combination of an adaptive array antenna and a canceller of interference for direct-sequence spread-spectrum multiple-access system," *IEEE J. Select. Areas Commun.*, vol. 8, pp. 675–682, May 1990.

[13] P. Patel and J. Holtzman, "Analysis of a simple successive interference cancellation scheme in a DS/CDMA system," *IEEE J. Select. Areas Commun.*, vol. 12, pp. 796–807, June 1994.

[14] A. Duel-Hallen, "A family of multiuser decision-feedback detectors for asynchronous code-division multiple-access channels," *IEEE Trans. Commun.*, vol. 43, pp. 421–434, Feb./Mar./Apr. 1995.

[15] S. Affes and P. Mermelstein, "A new receiver structure for asynchronous CDMA: STAR—The spatio-temporal array-receiver," *IEEE J. Select. Areas Commun.*, vol. 16, pp. 1411–1422, Oct. 1998.

[16] S. Affes, H. Hansen, and P. Mermelstein, "Interference subspace rejection in wideband CDMA: Modes for mixed-power operation," in *Proc. IEEE ICC'01, Communication Theory Symp.*, vol. 2, Helsinki, Finland, June 11–15, 2001, pp. 523–529.

[17] H. Hansen, S. Affes, and P. Mermelstein, "Interference subspace rejection in wideband CDMA: Modes for high data-rate operation," in *Proc. IEEE GLOBECOM'01*, vol. 1, San Antonio, TX, Nov. 25–29, 2001, pp. 475–479.

[18] M. F. Madkour, S. C. Gupta, and Y.-P. E. Wang, "A blind downlink blind interference cancellation in a W-CDMA mobile communications system," in *Proc. IEEE WCNC'99*, New Orleans, LA, Sept. 21–24, 1999, pp. 1119–1123.

[19] ——, "A subspace projection based blind interference cancellation scheme for W-CDMA downlink," in *Proc. 33rd Asilomar Conf. Signals, Systems, and Computers*, vol. 2, Pacific Grove, CA, Oct. 24–27, 1999, pp. 1611–1615.

[20] A. J. Viterbi, *CDMA Principles Spread Spectrum Communication*. Reading, MA: Addison-Wesley, 1995.

[21] K. Cheikhrouhou, S. Affes, and P. Mermelstein, "Impact of synchronization on performance of enhanced array-receivers in wideband CDMA networks," IEEE J. Select. Areas Commun., to be published.

[22] H. Hansen, S. Affes, and P. Mermelstein, "Interference subspace rejection in wideband CDMA: Modes for downlink operation," IEEE J. Select. Areas Commun., to be published.

[23] M. K. Varanasi and B. Aazhang, "Noncoherent decision-feedback multiuser detection," *IEEE Trans. Commun.*, vol. 48, pp. 259–269, Feb. 2000.

[24] S. Affes, A. Louzi, N. Kandil, and P. Mermelstein, "A high capacity CDMA array-receiver requiring reduced pilot power," in *Proc. IEEE GLOBECOM'2000, Communication Theory Symposium*, vol. 2, San Francisco, CA, Nov. 27–Dec. 1, 2000, pp. 910–916.

[25] A. C. Soong and W. Krzymien, "A novel CDMA multiuser interference cancellation receiver with reference symbol aided estimation of channel parameters," *IEEE J. Select. Areas Commun.*, vol. 14, pp. 1536–1547, Oct. 1996.

[26] S. Affes and P. Mermelstein, "Performance of a CDMA beamforming array-receiver in spatially-correlated Rayleigh-fading multipath," in *Proc. IEEE VTC'99*, vol. 1, Houston, TX, May 16–20, 1999, pp. 249–253.

[27] A. F. Naguib, "Adaptive Antennas for CDMA wireless networks," Ph.D. dissertation, Stanford Univ., Stanford, CA, 1996.

[28] S. Affes, S. Gazor, and Y. Grenier, "An algorithm for multisource beamforming and multitarget tracking," *IEEE Trans. Signal Processing*, vol. 44, pp. 1512–1522, June 1996.

[29] ——, "An algorithm for multisource beamforming and multitarget tracking—Further results," in *Proc. EURASIP EUSIPCO'96*, vol. I, Trieste, Italy, Sept. 10–13, 1996, pp. 543–546.

[30] S. Affes, H. Hansen, and P. Mermelstein, "Near–far resistant single-user channel identification by interference subspace rejection in wideband CDMA," in *Proc. IEEE SPAWC'01*, Taoyuan, Taiwan, R.O.C., Mar. 20–23, 2001, pp. 54–57.

[31] S. D. Gary, M. Kocic, and D. Brady, "Multiuser detection in mismatched multiple-access channels," *IEEE Trans. Commun.*, vol. 43, pp. 3080–3089, Dec. 1995.

[32] S. Parkvall, E. Ström, and B. Ottersten, "The impact of timing errors on the performance of linear DS-CDMA receivers," *IEEE J. Select. Areas Commun.*, vol. 14, pp. 1660–1668, Oct. 1996.

[33] M. Varanasi, "Parallel group detection for synchronous CDMA communication over frequency-selective Rayleigh fading channels," *IEEE Trans. Inform. Theory*, vol. 42, pp. 116–128, Jan. 1996.

[34] A. Klein, G. K. Kaleh, and P. W. Baier, "Zero forcing and minimum mean-square-error equalization for multiuser detection in code-division multiple-access channels," *IEEE Trans. Veh. Technol.*, vol. 45, pp. 276–287, May 1996.

[35] M. K. Tsatsanis and G. B. Giannakis, "Optimal decorrelating receivers for DS-CDMA systems: A signal processing framework," *IEEE Trans. Signal Processing*, vol. 44, pp. 3044–3055, Dec. 1996.

[36] M. Latva-aho and M. J. Juntti, "LMMSE detection for DS-CDMA systems in fading channels," *IEEE Trans. Commun.*, vol. 48, pp. 194–199, Feb. 2000.

[37] B. Abrams, A. E. Zeger, and T. E. Jones, "Efficiently structured CDMA receiver with near–far immunity," *IEEE Trans. Veh. Technol.*, vol. 44, pp. 1–13, Feb. 1995.

[38] H. Hansen, S. Affes, and P. Mermelstein, "Partial interference subspace rejection in CDMA systems," in *Proc. IEEE VTC'01*, vol. 3, Rhodes, Greece, May 6–9, 2001, pp. 1809–1813.

[39] ——, "A beamformer for CDMA with enhanced near–far resistance," in *Proc. IEEE ICC'99*, vol. 3, Vancouver, BC, Canada, June 6–10, 1999, pp. 1583–1587.

[40] M. Honig and M. Tsatsanis, "Adaptive techniques for multiuser CDMA receivers," *IEEE Signal Processing Mag.*, vol. 17, no. 3, pp. 49–61, May 2000.

[41] P. Patel and J. Holtzman, "Performance comparison of a DS/CDMA system using a successive interference cancellation (IC) scheme and a parallel scheme under fading," in *Proc. IEEE ICC'94*, New Orleans, LA, 1994, pp. 510–514.

[42] S. H. Hwang, C. G. Kang, and S. W. Kim, "Performance analysis of interference cancellation schemes for a DS/CDMA system under delay constraints," in *Proc. IEEE PIMRC'96*, 1996, pp. 569–573.
[43] E. S. Selby, *Standard Mathematical Tables*. Cleveland, OH: The Chemical Rubber Co., 1968.
[44] D. Koulakiotis and A. H. Aghvami, "Evaluation of a DS/CDMA multiuser receiver employing a hybrid form of interference cancellation in Rayleigh-fading channels," *IEEE Commun. Lett.*, vol. 2, pp. 61–63, Mar. 1998.
[45] S. Sun, L. K. Rasmussen, H. Sugimoto, and T. J. Lim, "A hybrid interference canceller in CDMA," in *Proc. IEEE ISSSTA'98*, vol. 1, 1998, pp. 150–154.
[46] S. Affes and Y. Grenier, "A source subspace tracking array of microphones for double talk situations," in *Proc. IEEE ICASSP'96*, vol. II, Atlanta, GA, May 7–10, 1996, pp. 909–912.
[47] L. K. Rasmussen, T. J. Lim, and A.-L. Johansson, "A matrix-algebraic approach to successive interference cancellation in CDMA," *IEEE Trans. Commun.*, vol. 48, pp. 145–151, Jan. 2000.
[48] D. Guo, L. K. Rasmussen, S. Sun, and T. J. Lim, "A matrix-algebraic approach to linear parallel interference cancellation in CDMA," *IEEE Trans. Commun.*, vol. 48, pp. 152–161, Jan. 2000.
[49] K. Jamal and E. Dahlman, "Multistage interference cancellation for DS-CDMA," in *Proc. IEEE VTC'96*, vol. 2, Atlanta, GA, Apr. 28–May 1 1996, pp. 671–675.
[50] C. Schlegel, S. Roy, P. D. Alexander, and Z. J. Xiang, "Multiuser projection receivers," *IEEE J. Select. Areas Commun.*, vol. 14, pp. 1610–1618, Oct. 1996.
[51] C. Schlegel, P. Alexander, and S. Roy, "Coded asynchronous CDMA and its efficient detection," *IEEE Trans. Inform. Theory*, vol. 44, pp. 2837–2847, Nov. 1998.
[52] X. Wang and H. V. Poor, "Blind equalization and multiuser detection in dispersive CDMA channels," *IEEE Trans. Commun.*, vol. 46, pp. 91–103, Jan. 1998.
[53] A. J. Paulraj and C. B. Papadias, "Space–time signal processing for wireless communications," *IEEE Signal Processing Mag.*, vol. 14, no. 6, pp. 49–83, Nov. 1997.
[54] T. Kawahara and T. Matsumoto, "Joint decorrelating multiuser detection and channel estimation in asynchronous CDMA mobile communications channels," *IEEE Trans. Veh. Technol.*, vol. 44, pp. 506–515, Aug. 1995.
[55] X. Wang and H. V. Poor, "Space–time multiuser detection in multipath CDMA channels," *IEEE Trans. Signal Processing*, vol. 47, pp. 2356–2374, Sept. 1999.
[56] M. C. Reed and P. D. Alexander, "Iterative multiuser detection using antenna arrays and FEC on multipath channels," *IEEE J. Select. Areas Commun.*, vol. 17, pp. 2082–2089, Dec. 1999.
[57] F.-C. Zheng and S. Barton, "Near–far resistant detection of CDMA signals via isolation bit insertion," *IEEE Trans. Commun.*, vol. 43, pp. 1313–1317, Feb./Mar./Apr. 1995.
[58] S. S. H. Wijayasuriya, G. H. Norton, and J. P. McGeehan, "A sliding window decorrelating receiver for multiuser DS-CDMA mobile radio networks," *IEEE Trans. Veh. Technol.*, vol. 45, pp. 503–521, Aug. 1996.
[59] J. Chuang, L. J. Cimini Jr., G. Y. Li, B. McNair, N. Sollenberger, H. Zao, L. Lin, and M. Suzuki, "High-speed wireless data access based on combining EDGE with Wideband OFDM," *IEEE Commun. Mag.*, vol. 37, pp. 92–98, Nov. 1999.
[60] W. C. Jakes, Ed., *Microwave Mobile Communications*. New York: Wiley, 1974.
[61] G. D. Forney Jr., "Maximum-likelihood sequence estimation of digital sequences in the presence of intersymbol interference," *IEEE Trans. Inform. Theory*, vol. 18, pp. 363–378, May 1972.

Sofiène Affes (S'94–A'95) received the Diplôme d'Ingénieur in electrical engineering, and the Ph.D. degree in signal and image processing from the École Nationale Supérieure des Télécommunications, Paris, France, in 1992 and 1995, respectively.

From 1995 to 1997, he was with INRS-Telecommunications, University of Quebec, Montreal, Canada, QC, as a Research Associate, then as an Assistant Professor until 2000. Currently, he is an Associate Professor in the Personal Communications Group. His research interests include statistical signal and array processing, synchronization, and multiuser detection in wireless communications. Previously, he was involved in the European ESPRIT projects 2101 ARS on speech recognition in adverse environments, in 1991, and 6166 FREETEL on hands-free telephony from 1993 to 1994. In 1997, he participated in the major program in personal and mobile communications of the Canadian Institute for Telecommunications Research. Since 1998, he has been leading the radio-design and signal processing activities of the Bell/Nortel/NSERC Industrial Research Chair in Personal Communications at INRS-Telecommunications.

Henrik Hansen was born in Copenhagen, Denmark, in 1971. He received the M.Sc. degree in communication engineering, and the Ph.D. degree in electrical engineering from the Technical University of Denmark, Lyngby, Denmark, in 1997 and 2001, respectively.

He since joined Ericsson, Denmark, as a UMTS radio-network designer. His research interests include digital modulation and coding, multiuser detection, interference cancellation, adaptive antennas, space–time processing, and radio-network optimization. From 1998 to 2000, he spent several doctoral leaves as a Visiting Researcher at INRS-Telecommunications, University of Quebec, Montreal, QC, Canada, working on multiuser detection. He is currently involved in the planning of future 3G radio networks at Ericsson, with a focus on the dimensioning of the air interface. He is also active in various research projects on wireless technologies.

Paul Mermelstein (S'58–M'63–SM'77–F'94) received the B.Eng. degree in engineering physics from McGill University, Montreal, Canada, and the S.M., E.E., and D.Sc. degrees in electrical engineering from Massachusetts Institute of Technology, Cambridge, in 1959, 1960, 1963, and 1964, respectively.

From 1964 to 1973, he was a member of the Technical Staff in the Speech and Communications Research Department, Bell Laboratories, Murray Hill, NJ. From 1973 to 1977, he was a member of the Research Staff at Haskins Laboratories, conducting research on speech analysis, perception, and recognition. From 1977 to 1994, he was with Bell Northern Research, in a variety of management positions, leading research and development activities in speech recognition, speech coding, and personal communications. From 1994 to 2000, he was the leader of the major program in personal and mobile communications of the Canadian Institute for Telecommunications Research. He currently holds the Bell/Nortel/NSERC Industrial Research Chair in Personal Communications at INRS-Telecommunications, University of Quebec, Montreal, QC, Canada. He is a past Associate Editor for Speech Processing of the Journal of the Acoustical Society of America.

Dr. Mermelstein was the Editor for Speech Communications of the IEEE TRANSACTIONS ON COMMUNICATIONS from 1985 to 1989.